On the Initiation of Metamorphic Sulfide Anatexis

ANDREW G. TOMKINS[1,2]*, DAVID R. M. PATTISON[1] AND B. RONALD FROST[3]

[1]DEPARTMENT OF GEOLOGY AND GEOPHYSICS, UNIVERSITY OF CALGARY, CALGARY, AB, CANADA T2N 1N4

[2]SCHOOL OF GEOSCIENCES, MONASH UNIVERSITY, PO BOX 28E, VIC. 3800, AUSTRALIA

[3]DEPARTMENT OF GEOLOGY AND GEOPHYSICS, UNIVERSITY OF WYOMING, LARAMIE, WY 82071, USA

Mineral assemblages in common sulfide ore deposits are examined together with phase relations to (1) investigate the pressure–temperature conditions required for the onset of metamorphically induced partial melting involving economic minerals, and (2) place constraints on the amount of melt produced. Deposits that contain sulfosalt or telluride minerals may start to melt at conditions ranging from lowest greenschist facies to amphibolite facies. Deposits lacking sulfosalt and/or telluride minerals may begin to melt once P–T conditions reach the upper amphibolite facies, if galena is present, or well into the granulite facies if galena is absent. The result is two broad melting domains: a low- to medium-temperature, low melt volume domain involving melting of volumetrically minor sulfosalt and/or telluride minerals; and a high-temperature, potentially higher melt volume domain involving partial melting of the major sulfide minerals. Epithermal gold deposits, which are especially rich in sulfosalt minerals, are predicted to commence melting at the lowest temperatures of all sulfide deposit types. Massive Pb–Zn (−Cu) deposits may start to melt in the lower to middle amphibolite facies if pyrite and arsenopyrite coexist at these conditions, and in the upper amphibolite facies if they do not. Excepting sulfosalt-bearing occurrences, massive Ni–Cu–PGE (platinum group element) deposits will show little to no melting under common crustal metamorphic conditions, whereas disseminated Cu deposits are typically incapable of generating melt until the granulite facies is reached, when partial melting commences in bornite-bearing rocks. The volume of polymetallic melt that can be generated in most deposit types is therefore largely a function of the abundance of sulfosalt minerals. Even at granulite-facies conditions, this volume is usually less than 0·5%. The exception is massive Pb–Zn deposits, where melt volumes significantly exceeding 0·5 vol. % may be segregated into sulfide magma dykes, allowing mobilization over large distances.

INTRODUCTION

Petrologists have a good understanding of the metamorphic conditions under which common crustal rocks start to melt and the chemical factors that influence the onset of partial melting, such as composition of fluid, minerals and bulk rock, yet there remains a class of minerals for which anatectic relationships are relatively poorly understood: the sulfides and sulfosalts that are concentrated in ore deposits.

Interpretations prior to 2001 involved two widely accepted mechanisms by which ore minerals could be remobilized during deformation and metamorphism of a sulfide ore deposit. These were solid state mechanical mobilization (where strain is preferentially partitioned into easily deformable sulfide minerals) and hydrothermal dissolution and reprecipitation (Marshall *et al.*, 2000). A third mechanism, partial melting and consequent remobilization of this melt, was proposed by Lawrence (1967) and Vokes (1971) for base metal deposits at Broken Hill, Australia, and Bleikvassli, Norway, respectively. However, some doubt was expressed over the validity of these early interpretations (Plimer, 1987; Skinner & Johnson, 1987). Metamorphic sulfide anatexis was discussed briefly by Marshall *et al.* (2000), but at the time only one deposit, Legenbach in Switzerland, had been shown to have partially melted (Hofmann, 1994; Hofmann & Knill, 1996; Knill, 1996).

*Corresponding author. Present address: School of Geosciences, Monash University, PO Box 28e, Vic. 3800, Australia. Telephone: +61 3 990 54879. Fax: +61 3 990 54903. E-mail: Andy.Tomkins@sci.monash.edu.au

Since 2001, it is being recognized, at an increasing number of metamorphosed sulfide ore deposits around the world, that part of the ore mineral assemblage underwent partial anatexis during metamorphism (Mavrogenes *et al.*, 2001; Tomkins & Mavrogenes, 2002; Tomkins *et al.*, 2004; Baile & Reid, 2005; Sparks & Mavrogenes, 2005; Ciobanu *et al.*, 2006). The ore minerals in these deposits that melted include sulfides, sulfosalts (containing As or Sb and S), tellurides and native minerals (metallic minerals lacking S and Te). Thus, an extensive range of minerals is referred to in this paper and abbreviations are presented in Table 1.

The metamorphic conditions inferred for these previously described deposits varied from $\sim520°C$, at the Lengenbach deposit in Switzerland (Hofmann, 1994), to as high as $850°C$ at the Challenger deposit in Australia (Tomkins & Mavrogenes, 2002). The lower end of this range shows that the onset of partial sulfide anatexis can occur at significantly lower temperatures than silicate partial melting. However, because large accumulations of sulfide minerals are rare, metamorphic partial sulfide anatexis is unlikely to have ever generated very large volumes of sulfide magma compared with silicate magmas. Nevertheless, understanding the processes behind sulfide partial melting during metamorphism is important for a range of reasons. During high-temperature metamorphism and deformation of sulfide ore bodies, even small proportions of sulfide melt are easily mobilized because their viscosities are very low (e.g. Dobson *et al.*, 2000). Further, the high viscosity contrast between solid sulfide minerals and sulfide melts implies that generally only melt will be mobilized and not a mixed liquid–solid mobilizate. This sulfide melt mobilization leads to development of complex mineralogical–structural associations that are impossible to interpret correctly if partial sulfide melting is not recognized (Tomkins *et al.*, 2004). Therefore, awareness that partial sulfide melting can occur facilitates a more accurate interpretation of ore body evolution, leading to better genetic models to be used in finding similar deposits. Understanding sulfide melt mobilization is also important to mine planning and near-mine exploration because segregation of even small amounts of sulfide magma can significantly redistribute ore metals, especially precious metals, in and around pre-existing mineral deposits (Tomkins & Mavrogenes, 2002; Tomkins *et al.*, 2004).

A number of important questions remain regarding metamorphically induced partial sulfide melting. (1) Under what metamorphic conditions do typical sulfide ore deposits start to melt? (2) Is this process capable of generating enough melt to be mobilized through sulfide magma veins and dykes over hundreds of meters or kilometers? (3) Can this process actually form new ore deposits? (4) Can our understanding of this process help us find undiscovered ore deposits?

The aim of this paper is therefore to explore the initial partial melting relationships in the common types of

Table 1: Mineral abbreviations used in this paper

Mineral	Abbreviation	Composition
Anilite	Anl	Cu_7S_4
Arsenopyrite	Asp	FeAsS
Bismuthinite	Bis	Bi_2S_3
Bornite	Bn	Cu_5FeS_4
Carrollite	Car	$Cu(Co,Ni)_2S_4$
Chalcocite	Cc	Cu_2S
Chalcopyrite	Cpy	$CuFeS_2$
Cinnabar	Cnb	HgS
Cobaltite	Cob	CoAsS
Covelite	Cov	CuS
Cubanite	Cub	$CuFe_2S_3$
Digenite	Dig	Cu_9S_8
Galena	Gn	PbS
Garnet	Grt	$(Fe,Mg,Mn,Ca)_3Al_2Si_3O_{12}$
Gudmundite	Gud	NiAsS
Molybdenite	Moly	MoS_2
Pentlandite	Pnt	$(Fe,Ni)_9S_8$
Pyrite	Py	FeS_2
Pyrrhotite	Po	$Fe_{1-x}S$
Sphalerite	Sph	ZnS
Stibnite	Stb	Sb_2S_3
Tennantite	Ten	$(Cu,Ag,Hg)_{10}(Fe,Zn,Cu,Hg)_2As_4S_{13}$
Tetrahedrite	Tet	$(Cu,Ag,Hg)_{10}(Fe,Zn,Cu,Hg)_2Sb_4S_{13}$
Quartz	Qtz	SiO_2

sulfide mineral deposits, and, in the process, gain an understanding of how much melt can be generated in various deposit types. A preliminary review of partial sulfide melting during metamorphism was conducted by Frost *et al.* (2002). Based primarily on an examination of textures at the Broken Hill Pb–Zn deposit in Australia (metamorphosed at granulite-facies conditions), those workers reviewed some of the published phase relations before developing a model for the formation of sulfide melts in massive Pb–Zn deposits. Five characteristic features were identified that may be used as evidence of partial sulfide melting, and then some other deposit types were briefly discussed as part of a section aimed at identifying additional partially melted ore deposits. The present study takes a more detailed look at the natural constraints on initial melting in all sulfide-bearing ore deposit types and attempts to constrain the proportions of melt generated as a function of natural conditions. This is achieved through bringing together previous experimental studies and observations of several ore deposits metamorphosed at conditions ranging from mid-amphibolite facies to granulite facies.

OVERVIEW OF CONDITIONS REQUIRED FOR SULFIDE MELTING

The temperature of sulfide melting

The most fundamental constraints on sulfide melting are provided by experimentalists, who have investigated phase relations in numerous systems relevant to sulfide ore deposits (almost all experiments were conducted at atmospheric pressures). These studies defined the melting temperatures for many individual ore minerals and more importantly, for many naturally occurring ore mineral assemblages. Table 2 lists the melting temperatures (T_m) for a range of naturally occurring ore minerals and mineral assemblages (the list is not complete because experimental data are lacking for many possible systems). This table summarizes the most basic melting relationships, and more detailed information is contained in numerous phase diagrams spread throughout the geological literature. Many of the relevant phase diagrams have been compiled by Tomkins *et al.* (2004).

Table 2 is broken into two parts to highlight the difference between melting of individual ore minerals in isolation and partial melting of coexisting ore minerals. In multiple mineral systems, the more minerals that coexist (i.e. are able to communicate chemically), the lower the initial partial melting temperature of the combination. For example, the melting temperature of gold is 1064°C, but if a small amount of bismuth is added, the combination partially melts at 375°C (at 1 bar; if >33 at. % Bi is added the melting point is even lower, at 241°C). Because Table 2 lists the melting temperatures of mostly individual minerals and binary systems, the actual initial partial melting temperatures of many natural ore assemblages, which have more coexisting minerals, are lower. The exception to this rule occurs where there is solid solution between two or more components in individual minerals. A good example is the system Sb_2S_3–PbS (stibnite–galena). Where a large ratio of Sb_2S_3 to PbS occurs, PbS is saturated in Sb_2S_3 and partial melting occurs at moderate temperatures (<550°C). In contrast, a low ratio of Sb_2S_3 to PbS (< ~3 mol % Sb_2S_3) results in a solid solution that does not melt until much higher temperatures are reached (far higher than the melting point of Sb_2S_3 alone), although the solid solution nevertheless melts at lower temperature than pure PbS (Salanci, 1979).

The information in Table 2 shows that numerous ore minerals melt at low temperatures, many of them within the greenschist facies. However, the minerals that melt at low temperatures are mostly rare sulfosalts as well as tellurides and some native minerals. In contrast, the sulfides melt at significantly higher temperatures.
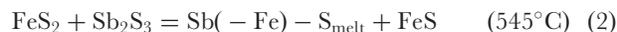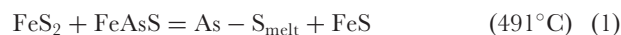
Factors affecting the temperature of sulfide melting

Pressure

In the few studies that have investigated the effects of pressure on partial sulfide melting reactions, it has been found that melting temperatures are only slightly affected by pressure. The eutectic temperature of the system pyrrhotite–galena–sphalerite increases by 6°C/kbar (Mavrogenes *et al.*, 2001), and the temperature of the reaction arsenopyrite + pyrite = As–S_{melt} + pyrrhotite increases by 14°C/kbar (Sharp *et al.*, 1985), whereas the temperature of the reaction jordanite = galena + Pb–As–S_{melt} does not vary with pressure (Roland, 1968). The influence of pressure on these reactions is shown in Fig. 1. The temperature of the eutectic in the system Fe–FeS has been studied at pressures ranging up to 60 kbar and it has been found to vary only slightly with changing pressure (see Brett & Bell, 1969; Ryzhenco & Kennedy, 1973; Usselman, 1975).

In S-absent native metal systems most elements melt at slightly higher temperatures with increased pressure. Bismuth and antimony are noteworthy for the fact that they melt at progressively lower temperatures with increased pressure (−4·5°C/kbar and −0·2°C/kbar respectively; Liu & Bassett, 1986). The effect of pressure on the melting temperature of telluride minerals remains unknown.

Sulfur and oxygen fugacity

Sulfur fugacity has an important influence on partial melting reactions that proceed with pyrite as a reactant. Some examples include

$$FeS_2 + FeAsS = As - S_{melt} + FeS \qquad (491°C) \quad (1)$$

$$FeS_2 + Sb_2S_3 = Sb(-Fe) - S_{melt} + FeS \qquad (545°C) \quad (2)$$

$$FeS_2 + PbS = Pb - Fe - S_{melt} + FeS \qquad (719°C) \quad (3)$$

$$FeS_2 + MoS_2 = Mo - Fe - S_{melt} + FeS \qquad (735°C). \quad (4)$$

The reactions are written for typical assemblages with pyrite in excess (the Fe in parentheses indicates that only 1–2% Fe occurs in the melt; all temperatures are at 1 bar). These reactions cannot proceed in rocks that maintain low fS_2 conditions during metamorphism because in such an environment pyrite is consumed at temperatures below those for the above reactions (Fig. 2; Toulmin & Barton, 1964; Craig & Vokes, 1993). Oxygen fugacity can exert a major influence on pyrite stability in deposits characterized by disseminated sulfide assemblages (see Tomkins *et al.*, 2006), such that low fO_2 conditions promote pyrite consumption during metamorphism (e.g. in graphite-bearing rocks), thus indirectly affecting sulfide melting. Although sulfur fugacities high enough for reactions (1) and (2) may be possible in a variety of natural rocks,

Table 2: The melting temperatures of minerals and mineral associations found in sulfide ore deposits

Mineral/association	Mineral formula	Melting T (°C @ 1 bar)	References
Sulfosalts, tellurides and native minerals			
Native mercury	Hg	−39	Liu & Bassett, 1986
Native bismuth	Bi	271	Liu & Bassett, 1986
Sartorite	$PbAs_2S_4$	305	Kutolglu, 1969
Orpiment	As_2S_3	310	Hansen & Aderko, 1958
Realgar	AsS	321	Hansen & Aderko, 1958
Maldonite	Au_2Bi	375	Okamoto & Massalski, 1986a
Baumhauerite	$Pb_3As_4S_9$	458	Kutolglu, 1969
Aurostibite	$AuSb_2$	460	Okamoto & Massalski, 1986b
Calaverite	$AuTe_2$	464	Okamoto & Massalski, 1986c
Pyrargyrite	Ag_3SbS_3	485	Bryndzia & Kleppa, 1988
Froodite	$PdBi_2$	485	Elliot, 1965
Michenerite$_{ss}$	(PdPt)BiTe	489–501	Cabri *et al.*, 1973
Miargyrite	$AgSbS_2$	510	Bryndzia & Kleppa, 1988
Tsumoite	BiTe	540	Elliot, 1965
Jamesonite	$Pb_4FeSb_6S_{14}$	545	Chang & Knowles, 1977
Zinkenite	$Pb_9Sb_{22}S_{42}$	546	Salanci, 1979
Jordanite	$Pb_{14}(As,Sb)_6S_{23}$	549	Roland, 1968
Chalcostibite	$CuSbS_2$	552	Bryndzia & Davis, 1989
Stibnite	Sb_2S_3	556	e.g. Bryndzia & Davis, 1989
Dyscrasite	Ag_3Sb	558	Hansen & Aderko, 1958
Robinsonite	$Pb_4Sb_6S_{13}$	583	Salanci, 1979
Tellurobismuthite	Bi_2Te_3	585	Elliot, 1965
Skinnerite	Cu_3SbS_3	610	Bryndzia & Davis, 1989
Sobolevskite	PdBi	620	Elliot, 1965
Tennantite	$Cu_{12}As_4S_{13}$	665	Maske & Skinner, 1971
Arsenopyrite	FeAsS	670	Clark, 1960
Kotulskite	Pd(Te,Bi)	720	Medvedeva *et al.*, 1961
Merenskyite	$(PdPt)(BiTe)_2$	740	Medvedeva *et al.*, 1961
Sulfides			
Cinnabar	HgS	825	Osadchii, 1990
Bornite	Cu_5FeS_4	840	Craig & Kullerud, 1967
Chalcopyrite	$CuFeS_2$	850	Craig & Kullerud, 1967
Galena	PbS	1114	Freidrich, 1907
Pyrrhotite	$Fe_{1-x}S$	1195	Freidrich, 1907
Sphalerite	ZnS	1680	Freidrich, 1907
Gold + native mercury	Au + Hg	−39	Okamoto & Massalski, 1986d
Gold + native bismuth	Au + Bi	241	Okamoto & Massalski, 1986a
Orpiment + lorandite$_{ss}$	$As_2S_3 + Tl(Sb,As)S_2$	<275	Sobott, 1984
Lorandite + stibnite	$TlAsS_2 + (Sb,As)_2S_3$	<275	Sobott, 1984
Orpiment + galena	$As_2S_3 + PbS$ (>44% As_2S_3)	∼300	Kutolglu, 1969
Orpiment + stibnite	$As_2S_3 + Sb_2S_3$	<310	Tomkins *et al.*, 2004
Orpiment + bismuthinite	$As_2S_3 + Bi_2S_3$ (>30% As_2S_3)	<310	Based on T_m of As_2S_3, see also Walia & Chang, 1973
Petzite + electrum	$AuAg_3Te_2 + AuAg_{ss}$	<335	Cabri, 1965
Gold + native antimony	Au + Sb (>45% Au)	360	Okamoto & Massalski, 1986b
Calaverite + altaite	$AuTe_2 + PbTe$	∼425	Prince *et al.*, 1990

Table 2: Continued

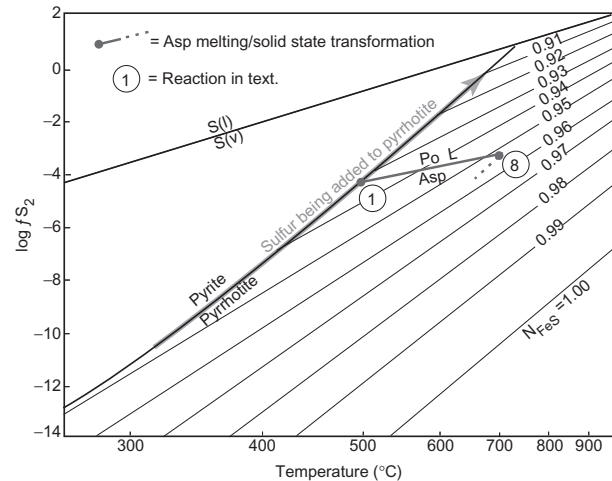| Mineral/association	Mineral formula	Melting T (°C @ 1 bar)	References
Gold + calaverite	$Au + AuTe_2$	447	Okamoto & Massalski, 1986c
Miargyrite + stibnite	$AgSbS_2 + Sb_2S_3$	450	Bryndzia & Kleppa, 1988
Pyrargyrite + argentite	$Ag_3SbS_3 + Ag_2S$	465	Bryndzia & Kleppa, 1988
Arsenopyrite + pyrite	$FeAsS + FeS_2$	491	Barton, 1969
Chalcostibite + stibnite	$CuSbS_2 + Sb_2S_3$	496	Bryndzia & Davis, 1989
Pyrite + stibnite	$FeS_2 + Sb_2S_3$	494–545	Barton, 1971
Pyrrhotite + stibnite	$FeS + Sb_2S_3$	550	Barton, 1971
Galena + argentite	$PbS + Ag_2S$	605	Urazov & Sokolova, 1983
Stibnite + bismuthinite	$Sb_2S_3 + Bi_2S_3$	556–764	Solid solution at high T; Springer & Laflamme, 1971
Pyrite + galena	$FeS_2 + PbS$	719	Brett & Kullerud, 1967
Py + Gn + Cpy + Sph	$FeS_2 + PbS + CuFeS_2 + ZnS$	~730 @ 2 kbar	Stevens et al., 2005
Pyrite + molybdenite	$FeS_2 + MoS_2$	735	Grover et al., 1975
Po + Gn + Sph	$FeS_{stoic.} + PbS + ZnS$	800	Mavrogenes et al., 2001
Bn + Po	$Cu_5FeS_4 + FeS$	<800	Tsujimura & Kitakaze, 2004
Bn + ISS	$Cu_5FeS_4 + CuFeS_2$	<800	Tsujimura & Kitakaze, 2004
Pyrrhotite + galena	$Fe_{1-x}S + PbS$	880	Freidrich, 1907
Sphalerite + galena	$ZnS + PbS$	1040	Freidrich, 1907
Pyrrhotite + sphalerite	$Fe_{1-x}S + ZnS$	1180	Freidrich, 1907
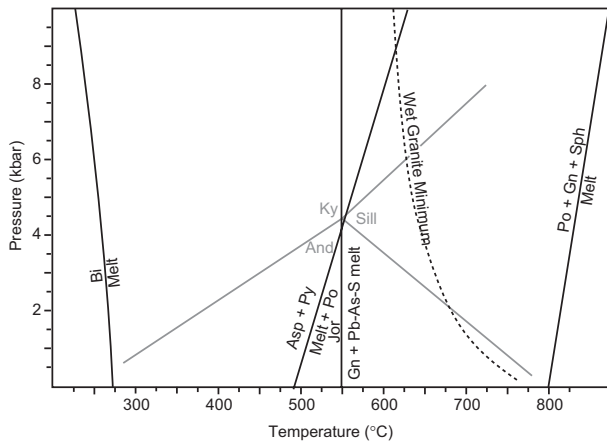
Fig. 1. The known pressure constraints on sulfide melting reactions. The position of the Al_2SiO_5 triple point and the wet granite curve are also shown for reference (obtained from Pattison, 1992; Spear, 1993).

Fig. 2. Log fS_2–T diagram showing the fS_2-dependent stability of pyrite and pyrrhotite and the compositional variation of pyrrhotite with fS_2 and temperature, at 1 bar. N_{FeS} is the mole fraction of FeS in the system FeS–S_2. Modified from Toulmin & Barton (1964).

the very high fugacities required for reactions (3) and (4) (Fig. 2) may be rare (Tomkins *et al.*, 2006).

Water and other hydrothermal phases

Water affects partial sulfide melting both directly and indirectly. Wykes & Mavrogenes (2005) showed that water induces a melting point depression in the system FeS–PbS–ZnS of 35°C (from 900°C to 865°C at 15 kbar), although they suggested that this effect may be muted at lower pressures. The effect of water on other sulfide systems remains unknown. Indirectly, at amphibolite-facies conditions and above, the presence of water requires consumption of pyrite to maintain equilibrium proportions of H_2S, SO_2 and S_2 in the fluid (Connolly & Cesare, 1993). As grade increases, increasing amounts of pyrite are consumed.

Little is known about whether other common components of the fluid phase such as CO_2, CH_4, H_2S, SO_2 and halogens have any direct effect on the melting temperatures of sulfide minerals. In a study on the chalcophile behaviour of halogens, Mungall & Brenan (2003) found that the melting point of monosulfide solid solution (mss) in the system Fe–Cu–Ni–S is lowered by the presence of Cl, and that Cl is progressively enriched in the melt during crystallization. Br and I, but not F, were also found to dissolve in small amounts in this system.

Comparison with silicate metamorphism

Figure 3 illustrates the conditions required for partial sulfide anatexis in relation to the classic metamorphic facies. Only a few key reactions out of the many listed in Table 2 are shown. The metamorphic facies boundaries come from Spear (1993), with the exception of the amphibolite–granulite facies boundary, which comes from Pattison *et al.* (2003).

Deposits that contain sulfosalts or tellurides may start to melt at conditions ranging from lowest greenschist facies to amphibolite facies, well below conditions required for partial melting of common silicate rocks. An important and potentially widespread reaction involves partial melting of pyrite + arsenopyrite at lower amphibolite conditions.

Deposits lacking sulfosalts and/or tellurides may begin to melt once *P*–*T* conditions reach the upper amphibolite facies, if galena and chalcopyrite are present, or well into the granulite facies, if galena is absent. Partial melting of another widespread and common sulfide association, chalcopyrite + pyrrhotite, does not occur within the range of normal metamorphism. However, partial melting of bornite + pyrrhotite or bornite + chalcopyrite commences at lower temperature ($\sim$800°C, at 1 bar), near the amphibolite–granulite facies boundary. Thus, there are two broad sulfide melting domains: a low- to medium-temperature, low melt volume domain involving the melting of minor sulfosalts and/or tellurides (this may involve complete melting of some phases and partial melting of others); and a high-temperature, potentially higher melt volume domain involving the partial melting of major sulfide minerals. The boundary between minor and major melting is depicted as a shaded band to reflect the effect of trace metals, as well as the possible effect of water, on lowering the eutectic melting temperature between the major sulfide minerals, galena + chalcopyrite + pyrrhotite + sphalerite. The lower temperature side of the band represents partial melting in the presence of water (35°C melting point depression; Wykes & Mavrogenes, 2005) and trace metals, whereas the upper temperature side represents partial melting in the absence of water and trace metals.

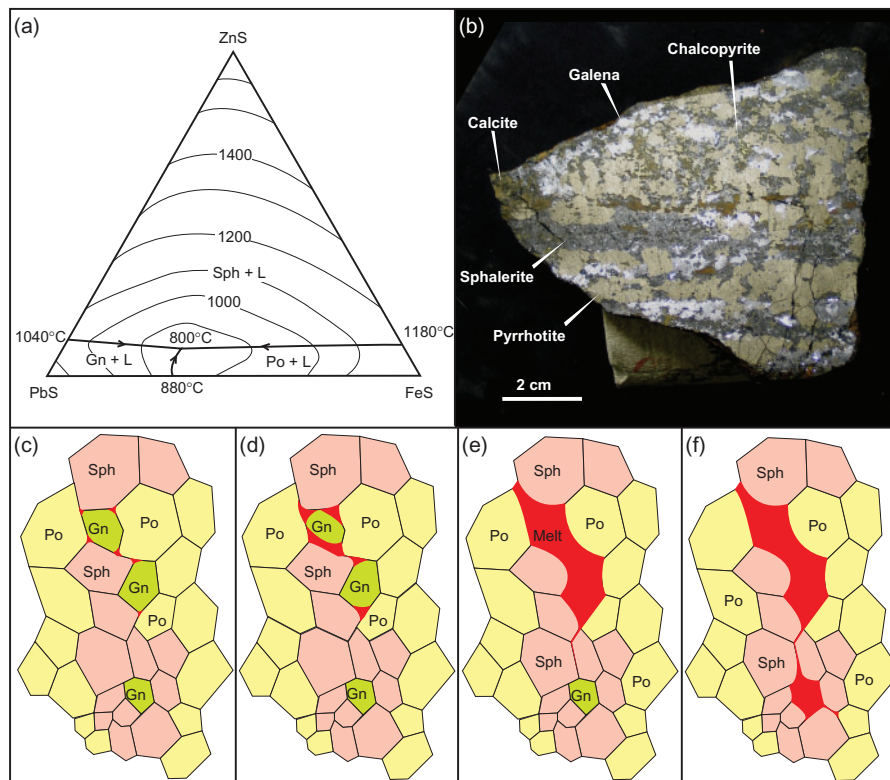## Mineral communication and mobilization-assisted melting

In any typical sulfide deposit each sulfide mineral will coexist with a variety of other minerals. The degree of chemical communication between the different minerals will affect the extent of melting. As an example, we may consider partial melting between galena, sphalerite and pyrrhotite (Fig. 4a). Within a given deposit, some galena grains might coexist with sphalerite only, others with pyrrhotite only, and still others with both sphalerite and pyrrhotite (Fig. 4b). As in most systems, partial melting occurs first where all three sulfide minerals coexist at a triple point, whereas there is no melting where only two coexist (Fig. 4c). Partial melting continues until all of one of the phases is consumed (in our example it is galena; Fig. 4d and e), at which point the melt is saturated in all three components and has a eutectic composition, which in this system is dominated by galena. As temperature rises above the eutectic temperature, sphalerite and pyrrhotite continue to partially melt, thereby remaining saturated in these phases. Because all of the galena at this locality has already been consumed, the melt is now no longer saturated in this mineral and the melt composition is now on the ZnS–FeS cotectic. If this galena-undersaturated melt is now mobilized it will melt enough of any galena that it comes in contact with to regain equilibrium (Fig. 4f). We refer to this last stage as mobilization-assisted melting.

Through mobilization-assisted melting a more diverse array of elements can be incorporated in the melt. For example, if the galena grain isolated within sphalerite in Fig. 4e was instead chalcopyrite, it too would be at least partly incorporated in the melt in Fig. 4f. Because adding more elements typically lowers the melting temperature, mobilization-assisted melting also allows more of the melt's saturated components (ZnS and FeS in the example) to be incorporated. It is clear that considerably more melt can be generated via this process.

A further important point to make is that sulfide ore deposits are not mineralogically homogeneous. Therefore, although mobilization-assisted melting acts to generate a more homogeneous melt composition, in reality the bulk compositions of local aliquots of sulfide melt across an entire deposit will vary considerably. Deposit-wide mineralogical variability also affects the volumes of melt that can be produced from different parts of a given deposit. Locally higher concentrations of the low melting point minerals and elements, a natural consequence of the original hydrothermal mineralizing process, will produce locally higher melt volumes. Thus, although on average only 1% of the deposit may melt (for example), the local melt proportion at small scales might exceed 10%. This applies to all sulfide deposits that melt.
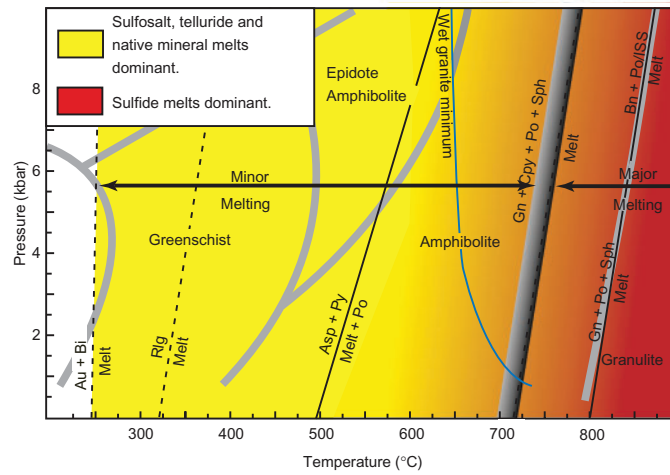
Fig. 3. The temperature–pressure range over which sulfosalts, tellurides, native minerals and sulfides melt. Continuous black lines indicate that pressure constraints are known; dashed black lines indicate that the effect of pressure is unknown. Wide grey lines separate the metamorphic facies [the amphibolite to granulite transition is from Pattison et al. (2003) and the other facies boundaries are from Spear (1993)]. The wide band separating minor from major melting represents the variation caused by differences in the natural environment in the amount of H_2O present (Wykes & Mavrogenes, 2005), and in the amount of trace metals present, on an assemblage containing galena + chalcopyrite + pyrrhotite + sphalerite. There will be widespread melting of the major sulfides at lower temperatures in wet, trace metal-rich rocks. The melting curve of galena + troilite (stoichiometric FeS) + sphalerite plots in the same position as that for bornite + ISS and bornite + pyrrhotite ($Fe_{1-x}S$).

Fig. 4. The influence of mineral communication and mobilization-assisted melting on the volume of melt that can be generated during metamorphism. (a) PbS–FeS–ZnS phase diagram modified from Mavrogenes et al. (2001). The diagram is drawn for conditions of 1 bar; however, Mavrogenes et al. (2001) showed that at 5 kbar the eutectic temperature is ∼800°C when natural pyrrhotite compositions are used and when the system is doped with trace silver. (b) Photograph of massive sulfides containing pyrrhotite, galena, sphalerite and chalcopyrite from the Bluebell mine (B.C., Canada), showing the level of chemical communication between the sulfides in a natural sample. (c–f) A series of sketches depicting incipient melting progressing to mobilization-assisted melting in the system PbS–$Fe_{1-x}S$–ZnS involving galena (Gn), sphalerite (Sph) and pyrrhotite (Po).

EARLIEST MELTING IN SULFIDE ORE DEPOSITS

We have categorized the various types of sulfide ore deposits into four general groups: massive Pb–Zn ± Cu deposits; gold deposits; magmatic Ni–Cu–PGE (platinum group element) deposits; disseminated Cu deposits. These groups are split into the more well-known ore deposit types and the typical sulfide mineral assemblages found in each type are listed in Table 3. This organization provides a geochemical framework for our analysis of initial melting within each of the four general groups. Several highly metamorphosed ore deposits of different types have been investigated to provide a basis for theoretical discussions on the conditions of initial melting in sulfide mineral deposits, and the volumes of melt expected to be generated. The location of these deposits is shown in Fig. 5.

Massive Pb–Zn ± Cu deposits
Observations

The Lengenbach deposit (Switzerland) is a Pb–Zn-rich massive sulfide deposit that has been shown to have partly melted during moderate-temperature metamorphism at

Table 3: The mineralogy of sulfide ore deposits

Ore deposit type	Typical initial mineralogy premetamorphism	Dominant minerals involved in initial melting	Initial T_m (mineralogy dependent)
Massive Pb–Zn (Cu) deposits			
VMS	Py, Po, Sph, Gn, Cpy (Asp)	Asp, Py	Asp + Py: ~560°C @ 5 kbar;
SEDEX	Py, Sph, Gn (Cpy, Asp)	Asp, Py	Gn + Cpy + Po + Sph: ~730°C @ 2 kbar
MVT	Gn, Sph, Py (Cpy, Asp)	Asp, Py	
Gold deposits			
Alluvial Au	Au (Ag in solid solution)	Au–Ag$_{ss}$	No melting
Epithermal Au–Ag	Py, numerous sulfosalts, tellurides, Au, electrum, Cnb, Cpy, Sph, Gn, native Hg	Sulfosalts, tellurides	<350°C @ 1 bar
Carlin-type Au	Arsenian Py (Au, trace Tl-sulfosalts), Cnb, Tet–Ten$_{ss}$, Cu–Zn–Pb sulfides	Tl-sulfosalts	<300°C @ 1 bar
Sb-rich Au	Stb, Asp, Py, Au	Stb, Asp, Py	Stb: 556°C @ 1 bar; Asp + Py: ~560°C @ 5 kbar
Mesothermal Au	Py, Po, Asp, tellurides, Au, Cpy, native Bi	Asp, tellurides, native Bi	Au + Bi: 241°C @ 1 bar; Au–Ag tellurides: <350°C @ 1 bar; Asp + Py: ~560°C @ 5 kbar
Magmatic Ni–Cu–PGE deposits			
	Po, Pnt, Cpy (Cub, Py, sulfarsenides, arsenides, bismuthotellurides)	Bi-tellurides	<500°C @ 1 bar
Disseminated copper deposits			
Cu–Au–(Mo) porphyry	Cpy, Bn, Moly, Py (Tet–Ten, enargite, Sph, Gn, Au)	Tet–Ten$_{ss}$	Tet–Ten$_{ss}$: ~485–650°C @ 1 bar (composition dependent); Bn + Cpy: ~800°C @ 1 bar
Skarns	Cpy, Moly, Py, Po, Sph, Gn—all variable (Au, Asp, Bi, Bis, Bn, tellurides)	Native Bi, tellurides, Asp + Py	Au + Bi: 241°C @ 1 bar; Au–Ag tellurides: <350°C @ 1 bar; Asp + Py: ~560°C @ 5 kbar
Fe-oxide Cu–Au–U	Py, Cpy, Bn, Cc (Cov, Car, Sph, Au, Cob)	Cpy, Bn	Bn + Cpy: ~800°C @ 1 bar
Sediment-hosted stratiform Cu	Cc, Bn, Cpy, Py (Gn, Sph, Cu, Dig, Cov, Anl, trace sulfosalts in some deposits)	sulfosalts, Cpy, Gn	lower amphibolite facies (sulfosalts); Gn + Cpy + Po + Sph: ~730°C @ 2 kbar

In the typical initial mineralogy column, the minerals in parentheses are minor or trace minerals. Mineralogy varies between individual deposits within each deposit type. Abbreviations are as listed in Table 1. Initial melting is based on published phase relations discussed in the text and listed in Table 2.
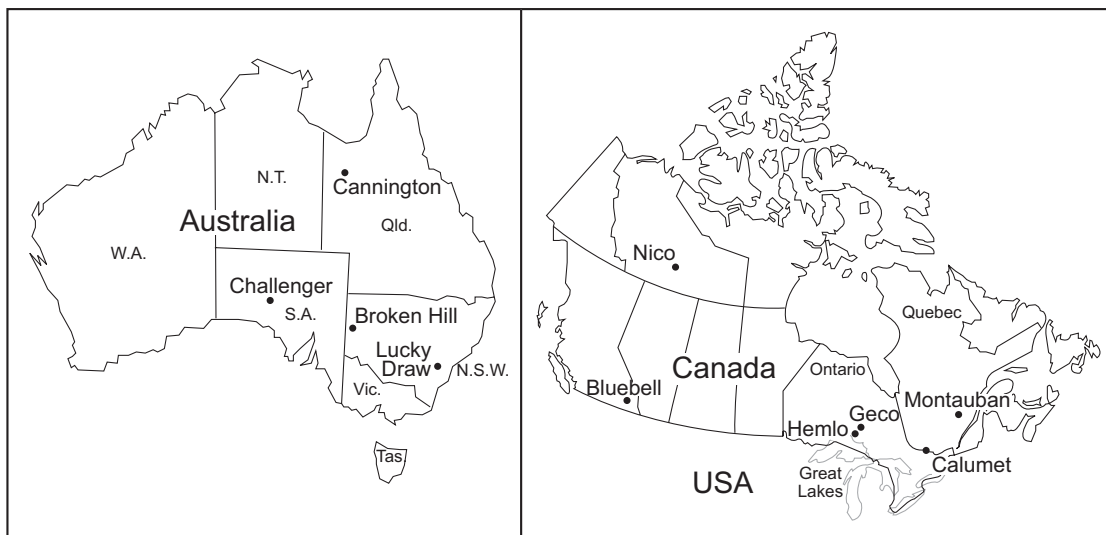
Fig. 5. Location of mineral deposits discussed in this study.

approximately 520°C (Hofmann, 1994; Hofmann & Knill, 1996). It has an unusually Tl- and As-rich assemblage that is not typical of this group of deposits. We have investigated two more intensely metamorphosed deposits that contain massive Pb–Zn ± Cu sulfide assemblages, the Broken Hill and Montauban deposits. The Broken Hill deposit (New South Wales, Australia) was metamorphosed at granulite-facies conditions of approximately 800–850°C and 5 kbar (see Phillips, 1980; Stevens *et al.*, 1988; Cartwright, 1999; Frost *et al.*, 2005) and has been previously demonstrated to have partly melted (Mavrogenes *et al.*, 2001; Frost *et al.*, 2005; Sparks & Mavrogenes, 2005). The Montauban deposit (Quebec, Canada; Stamatelopoulou-Seymour & MacLean, 1984) was metamorphosed at middle to upper amphibolite-facies conditions (650°C, 5 kbar; Bernier *et al.*, 1987). Possible arsenopyrite melting at Montauban and at two additional deposits (Geco and Osborne Lake mines, both in Canada) was discussed by Tomkins *et al.* (2006), and several other deposits where partial sulfide melting may have taken place were identified by Frost *et al.* (2002).

In Fig. 6 back-scattered electron (BSE) images of mineral associations from Broken Hill and Montauban are presented, which may be interpreted as crystallized accumulations of melt when the assemblage and metamorphic conditions are considered together. Experimental verification of this interpretation at Montauban is described below. These examples all come from small fractures in the wall rock adjacent to the massive sulfide units. An important characteristic of each is the abundance of sulfosalts and, in some, native minerals, relative to the volumetrically dominant massive sulfide minerals. The examples in Fig. 6 are highly enriched in elements such as Sb, As, Bi, Ag, Au and Pb, but depleted in Zn and Fe when compared with the bulk composition of the massive sulfide unit.

Several samples from each deposit contain numerous inclusions, fractures and intergranular aggregations filled with these sulfosalts, sulfides and native minerals. In several of these samples we have attempted to measure and calculate local bulk compositions of a statistically significant number of accumulations. This was done by taking a BSE image of each accumulation and obtaining a wavelength-dispersive spectromety (WDS) analysis of each mineral in the accumulation using the JEOL JXA8200 electron microprobe at the University of Calgary. Approximate bulk compositions of each accumulation were obtained using image analysis techniques within Adobe Photoshop to calculate the area of each analysed mineral in each BSE image. This technique cannot provide an exact local bulk composition because we can only ever view a two-dimensional section through each sulfosalt accumulation. Figure 7 shows a variation diagram produced from these data for a sample from the Montauban deposit (the same sample as used in the experiment described in the next section). There is an inverse correlation between the amount of Pb (as PbS) in each accumulation and the amount of Sb, As, Ag, and Au.

An experimental test of sulfide melting at the Montauban deposit

To test if native mineral–sulfosalt–sulfide accumulations at the Montauban deposit were once melts, a natural sample was held at temperature and pressure approximating peak metamorphic conditions in a Boyd & England (1960) type
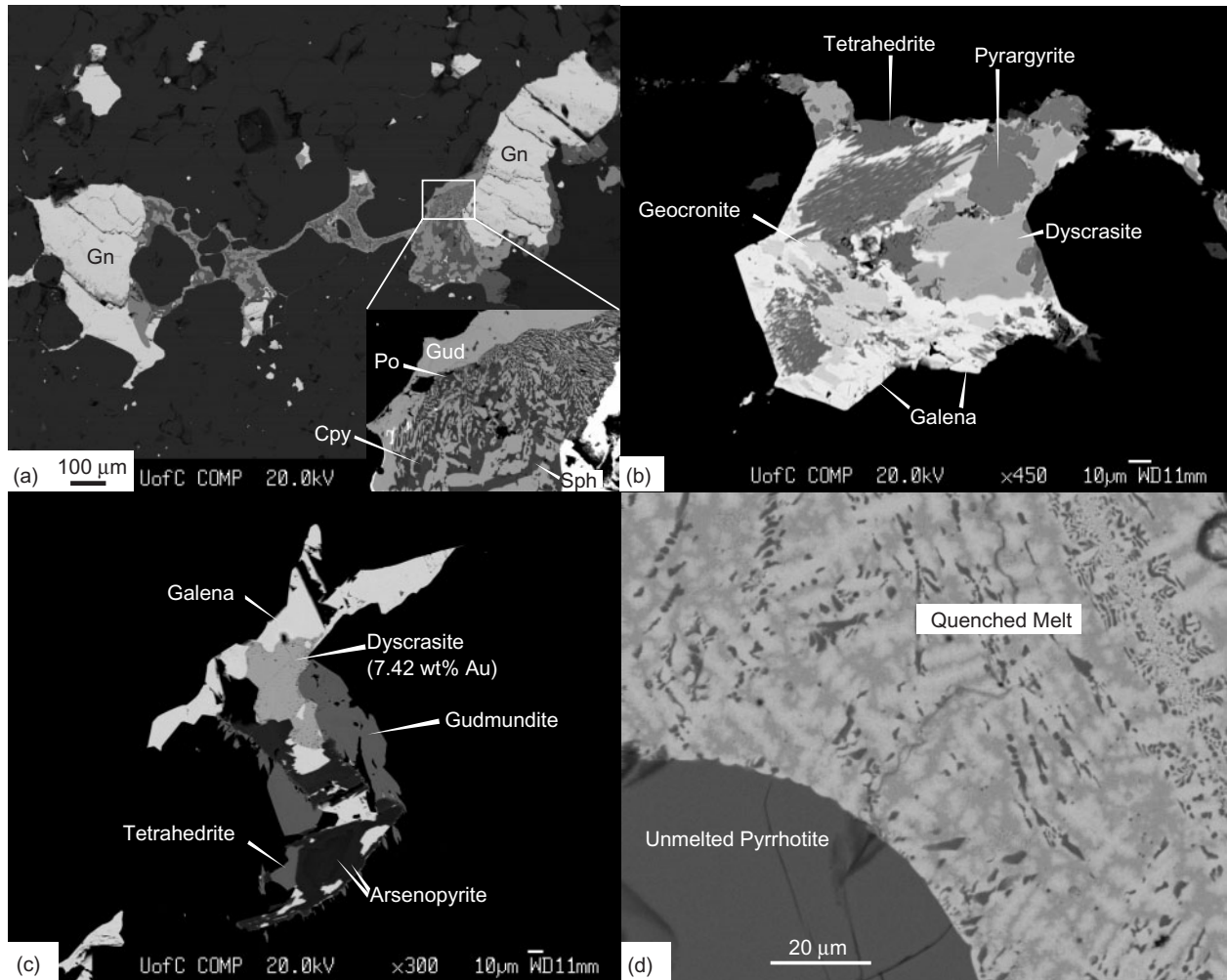
Fig. 6. Mineral associations from massive Pb–Zn(–Cu) deposits interpreted to represent crystallized accumulations of sulfide melt. (a) Gudmundite (FeSbS; Gud) in association with galena (Gn), pyrrhotite (Po), sphalerite (Sph) and chalcopyrite (Cpy) in a fracture in garnetite (wall-rock) from the Broken Hill deposit. The intimately mixed texture involving gudmundite and pyrrhotite may be indicative of simultaneous crystallization during cooling along a cotectic. (b, c) Sb–Ag-rich accumulations of sulfosalts, sulfides and native minerals from the Montauban deposit. Although Sb and Ag may be accommodated in galena as a coupled substitution, the abundance of these elements relative to galena in the examples suggests that the assemblage would have been molten during peak metamorphism. (d) The result of an experiment (run at 650°C, 5 kbar) conducted on the sample that contained (b) and (c). The SEM BSE image shows unmelted pyrrhotite and an intimately mixed mosaic of PbS, FeS and an Ag–Pb–Sb–S phase; the mixed area representing quenched melt.

piston cylinder apparatus (the experiment was conducted at the Research School of Earth Sciences at the Australian National University). One half the sample shown in Fig. 7 was polished and examined by reflected light microscopy to confirm that the sample used in the experiment contained numerous native mineral–sulfosalt–sulfide accumulations. The other half of the sample was shaped to fit inside a graphite sleeve. The sample and graphite sleeve were then encased in a talc sleeve. A corundum disc separated the sample from a thermocouple and boron nitride (BN) plugs fitted into both ends of the sleeves. The thermocouple, inserted through one of the BN plugs, allowed temperature readings from within 0·5 mm of

the sample. This assembly was held in the piston cylinder apparatus at 650°C and 5 kbar, the estimated metamorphic conditions of the deposit, for 24 h and then quenched. The experiment product was analysed using reflected light and electron microscopy.

Metallic and sulfide melts do not quench to glasses, but crystallize on quenching to a microcrystalline intergrowth of phases (e.g. Sparks & Mavrogenes, 2005). In contrast, unmelted material remains as coarse individual grains that are not mixed with other material. Gravity separation of melt from residuum in experiments by Stevens *et al.* (2005) showed that these quench textures indicate the presence of a sulphide melt. Observation of these quench
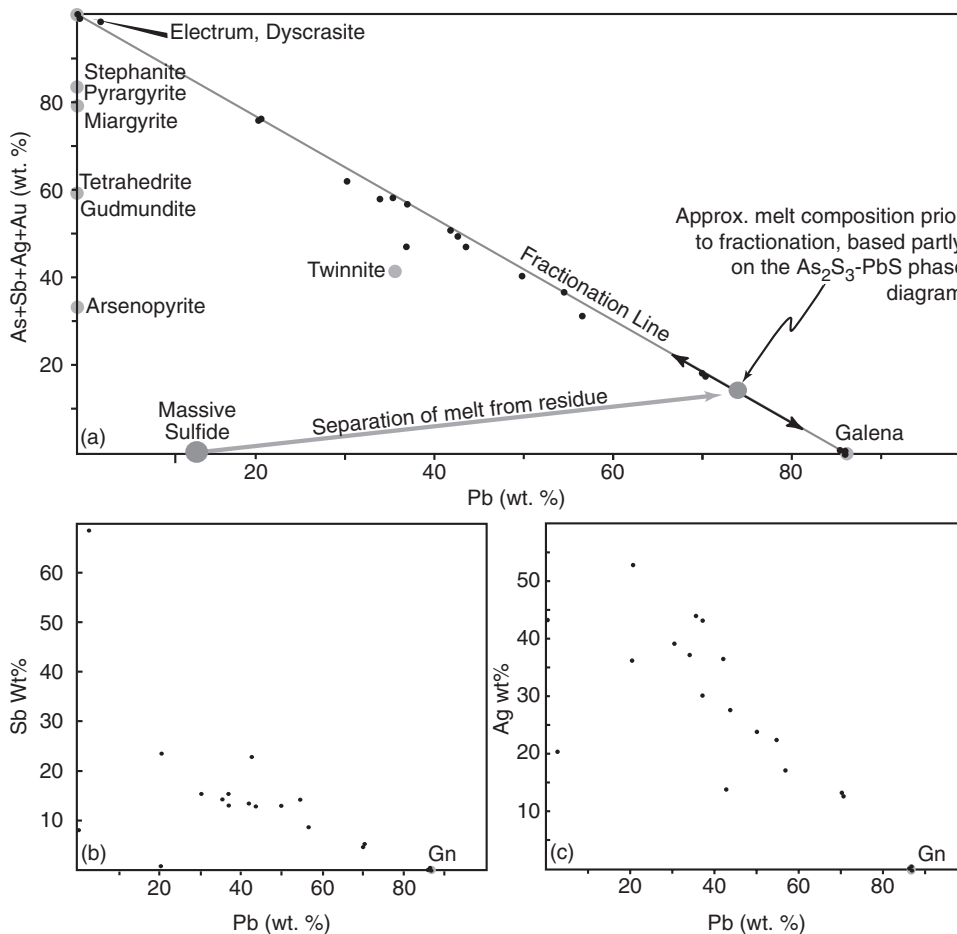
Fig. 7. Variation diagrams for a sample from the Montauban deposit. (a) Wt % As + Sb + Ag + Au plotted against wt % Pb. Also shown are the compositional positions of sulfosalts that crystallized from the interpreted melt. (b) Wt % Sb plotted against wt % Pb. (c) Wt % Ag plotted against wt % Pb. The data in these diagrams have been normalized to remove the pyrrhotite component from the bulk analysis. This was done because pyrrhotite was very probably in the rock prior to addition of sulfide melt and there is textural evidence that the melt has reacted with this pre-existing pyrrhotite to produce various Fe-bearing sulfosalts.

textures in the experiment product is therefore taken as evidence that the accumulations in question were once at least partly molten. Analyses by reflected light and electron microscopy of the experiment product show quench textures (Figs. 6d), which indicate that the native mineral–sulfosalt–sulfide accumulations from the Montauban deposit were at least partly molten at the estimated metamorphic conditions. This therefore suggests that a small proportion of melt containing Ag, As, Au, Pb, Sb and S was present during peak metamorphism.

Mineralogical constraints on initial melting

The ore mineral assemblage in volcanogenic massive sulfide (VMS), Mississippi Valley type (MVT), and sedimentary exhalative (SEDEX) type deposits is typically dominated by some combination of pyrite, pyrrhotite, sphalerite, galena and chalcopyrite (in this section we use chemical formulae when discussing

experiments and mineral names when discussing natural minerals). Based on an experimental study in the system $CuFeS_2$–PbS–FeS–ZnS–S conducted at 2 kbar, it has been suggested that where these minerals coexist they may start to melt at temperatures between 700 and 730°C (Stevens *et al.*, 2005). In an early study conducted at atmospheric pressures, Craig & Kullerud (1967) suggested that $CuFeS_2$ + PbS start to melt at ∼630°C. Our observations of textures in ore deposits suggest that the Stevens *et al.* (2005) study is more accurate; coexisting galena and chalcopyrite appear stable at Montauban, whereas chalcopyrite is a common component of the Broken Hill melts. Consequently, the Stevens *et al.* (2005) data are listed in Table 2 and shown in Fig. 3.

However, in many deposits galena and chalcopyrite do not occur together. In the absence of chalcopyrite and any minor phases, partial melting may not occur until temperatures of ∼800°C (at 5 kbar) are reached, when
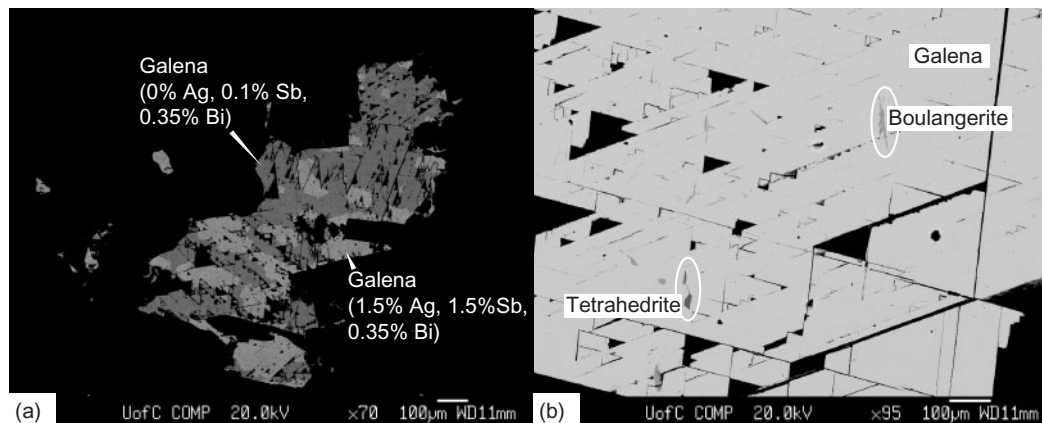
Fig. 8. Textural evidence of Ag, Sb, and Bi solid solution in galena. (a) Patchy zoning in galena from the Montauban deposit, highlighting Ag-, Sb- and Bi-rich zones (brighter) and Ag-, Sb- and Bi-poor zones (darker). (b) Exsolutions of boulangerite ($Pb_5Sb_4S_{11}$) and Ag-tetrahedrite $[(Ag,Cu)_{10}(Cu,Fe,Zn)_2(As,Sb)_4S_{13}]$ in galena from the Geco deposit. Other observed exsolution minerals include native Bi, native Ag, dyscrasite (Ag_3Sb) and diaphorite ($Pb_2Ag_3Sb_3S_8$).

galena + sphalerite + pyrrhotite + H_2O (+trace Ag) start to melt (Mavrogenes *et al.*, 2001; Wykes & Mavrogenes, 2005). In galena-free massive sulfide assemblages containing pyrrhotite, chalcopyrite and sphalerite, partial melting may not occur within the limits of typical crustal metamorphism. Although the eutectic temperature in this system has never been determined by experimentalists, Kojima & Sugaki (1984) indicated extensive solid solution fields at 800°C (at 1 bar). However, some minor sulfide and sulfosalt phases do occur in many of these deposits and they may be critical to the low-temperature generation of small quantities of melt.

In many occurrences, minor Sb-, Bi- and Ag-bearing sulfosalt minerals appear to have formed during cooling, as these elements exsolved from galena, with which they are commonly associated (Fig. 8a and b). Figure 9 shows the large extent of coupled substitution of Ag^+–Sb^{3+} and Ag^+–Bi^{3+} for $2Pb^{2+}$ in PbS (e.g. Blackburn & Schwendeman, 1977). Given the typically low concentrations of Sb, Bi and Ag in these deposits relative to Pb (ores typically contain <0·1% Ag, Sb and Bi, but percent levels of Pb as galena), it is likely that all would substitute into galena during metamorphism without causing any partial melting. However, Sb-, Bi- and Ag-doped PbS starts to melt at lower temperatures than pure PbS, when combined with other sulfide minerals (e.g. Mavrogenes *et al.*, 2001).

One mineral that typically occurs in minor amounts in these deposits and that cannot form as an exsolved mineral during cooling is arsenopyrite. In contrast to Sb, Bi and Ag, there is no known solid solution of As in PbS (Fig. 10). Arsenopyrite can partly melt during metamorphism through reaction (1), when high fS_2 conditions are generated through decomposition of pyrite. Reaction (1) occurs at 491°C at 1 bar and ~560°C at 5 kbar (Clark, 1960;

Sharp *et al.*, 1985). This and several other metamorphic processes that can also lead to formation of As–S melt from arsenopyrite breakdown have been discussed extensively by Tomkins *et al.* (2006). Because there is no substitution of As in PbS, the presence of small quantities of As–S melt causes partial melting of galena at temperatures as low as ~549°C (at 1 bar), the melting point of $Pb_{14}(As,Sb)_6S_{23}$ (jordanite; Fig. 10). Experiments by Roland (1968), conducted at pressures of up to 2 kbar, found that the melting point of $Pb_{14}(As,Sb)_6S_{23}$ (jordanite) was not affected by pressure within the uncertainty of measurement. It should be noted that Fig. 10 does not represent the phase relations exactly because the As–S melt produced through arsenopyrite melting does not have the composition As_2S_3; it has a composition that has slightly less sulfur than arsenic (Tomkins *et al.*, 2006). The ternary phase relations in the system As–Pb–S (Roland, 1968) suggest that this should not greatly affect the topology of the phase diagram above 550°C (see Tomkins *et al.*, 2006, fig. 4). The amount of PbS that melts when combined with an As–S melt of appropriate composition should be slightly greater than as represented by Fig. 10 (as suggested by the dashed liquidus surface on the right of the diagram).

Other minor As-bearing sulfosalts may also melt at mid-amphibolite-facies temperatures (e.g. Maske & Skinner, 1971), but in these deposits these minerals are typically rare compared with arsenopyrite. At middle amphibolite-facies conditions (*c*. 550–700°C), interaction between As–S melt and PbS results in extensive partial melting of the latter (Fig. 10). For example, at 650°C (and 1 bar) 1 mole of As–S melt will cause at least 3·8 moles of PbS to melt. However, typical bulk compositions in massive sulfide deposits have a very large ratio of galena to arsenopyrite, so the As–S melt would become saturated in galena,
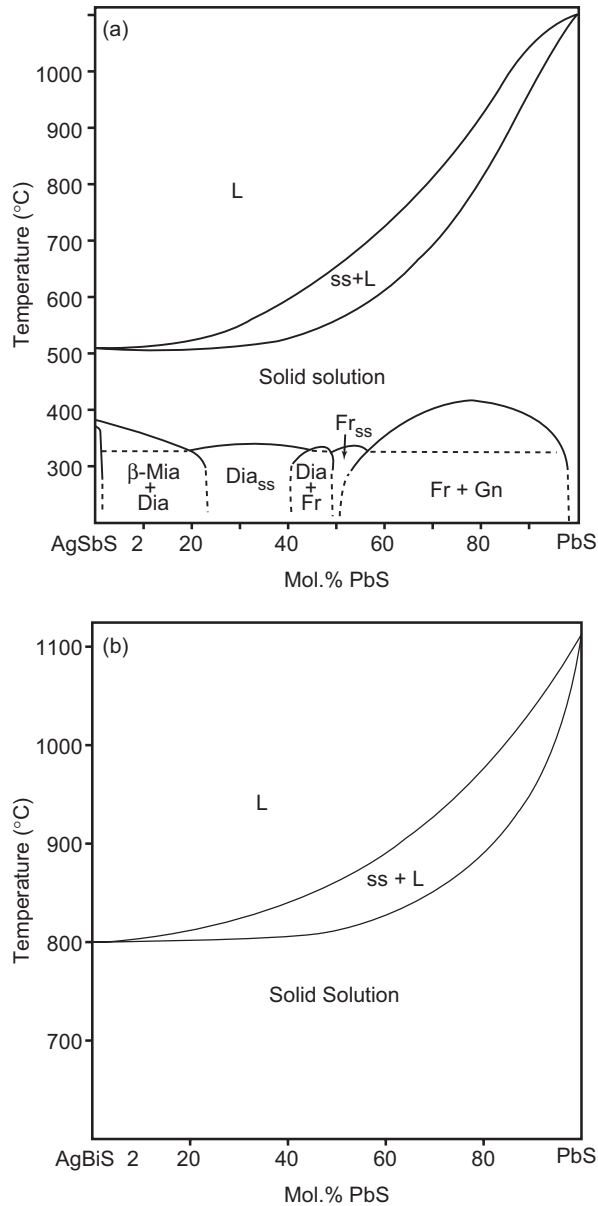
Fig. 9. Phase diagrams showing the extent of coupled substitution of Ag^+–Sb^{3+} (a) (modified from Hoda & Chang, 1975) and Ag^+–Bi^{3+} (b) (modified from Van Hook, 1960) for $2Pb^{2+}$ in galena.

and most of the galena would not melt. Nevertheless, it is of interest to know how much melt might be generated in these deposits as a result of the presence of minor arsenopyrite.

Volume of melt generated during initial melting

We have derived an equation to estimate the amount of As–Pb–S melt present in any given galena-bearing rock (above 549°C) using the arsenic content from bulk-rock analysis (based on Fig. 10). First, the amount of As–S melt from arsenopyrite breakdown is calculated; the amount of

sulfur required is calculated from the As–S phase diagram (Massalski *et al.*, 1990), assuming that the As–S melt composition is on the liquidus in this system (see Tomkins *et al.*, 2006):

$$\text{wt \% As} - \text{S}_{\text{melt}} = \frac{As + As((0\cdot01\,T - 19)/ - 63\cdot259)}{10\,000}$$
$$= \frac{As - 0\cdot016As(0\cdot01\,T - 19)}{10\,000}$$

(5)

where As is the As content of the rock (in ppm) and T is the temperature in °C.

Then, the amount of PbS incorporated by the As–S melt is calculated by fitting a curve to a graph of moles of PbS melted vs temperature, according to the phase diagram (Fig. 10) of Kutolglu (1969):

$$\text{wt \% PbS}_{\text{melt}} = \frac{239\cdot65X_{\text{As}}(3\cdot92 \times 10^{-22} \cdot T^{75} + 3\cdot27)}{10\,000}$$

(6)

where $X_{\text{As}} = \text{As}/74\cdot922$ (239·65 and 74·922 are the atomic weights of PbS and As, respectively).

Finally, these are incorporated into one formula and converted to volume percent:

$$\text{vol. \% melt} = \left[\frac{As - 0\cdot016As(0\cdot01\,T - 19)}{10\,000}\right]\left(\frac{D}{3560}\right)$$
$$+ \left[\frac{239\cdot65X_{As}(3\cdot92 \times 10^{-22} \cdot T^{75} + 3\cdot27)}{10\,000}\right]$$
$$\left(\frac{D}{7580}\right)$$

where D is the density of the whole rock (in kg/m³).

Simplifying,

$$\text{vol. \% melt} = As \cdot D(1\cdot66 \times 10^{-29}\,T^{75}$$
$$- 4\cdot49 \times 10^{-12}\,T + 1\cdot75 \times 10^{-7}).$$

(7)

Based on the experiments of Roland (1968), the effect of pressure is likely to be minor. The density of the As–S component of the melt is assumed to be ~3560 kg/m³ and that of the Pb–S component to be ~7580 kg/m³, based on the density of realgar and galena, respectively. The result represents the maximum amount of As–Pb–S melt that can exist, assuming that all of the As in the rock forms a melt and that all As–S melt can communicate chemically with excess galena. In many rocks these are not valid assumptions (see Tomkins *et al.*, 2006) and care should be taken when applying this formula. Table 4 shows the results of this calculation performed on a range of ore deposits. It can be seen that although the overall As content of massive Pb–Zn deposits is typically low, a significant melt fraction can be generated locally in As-rich portions of the deposit if all of the As in the rock forms a melt. It should be noted that this calculation considers
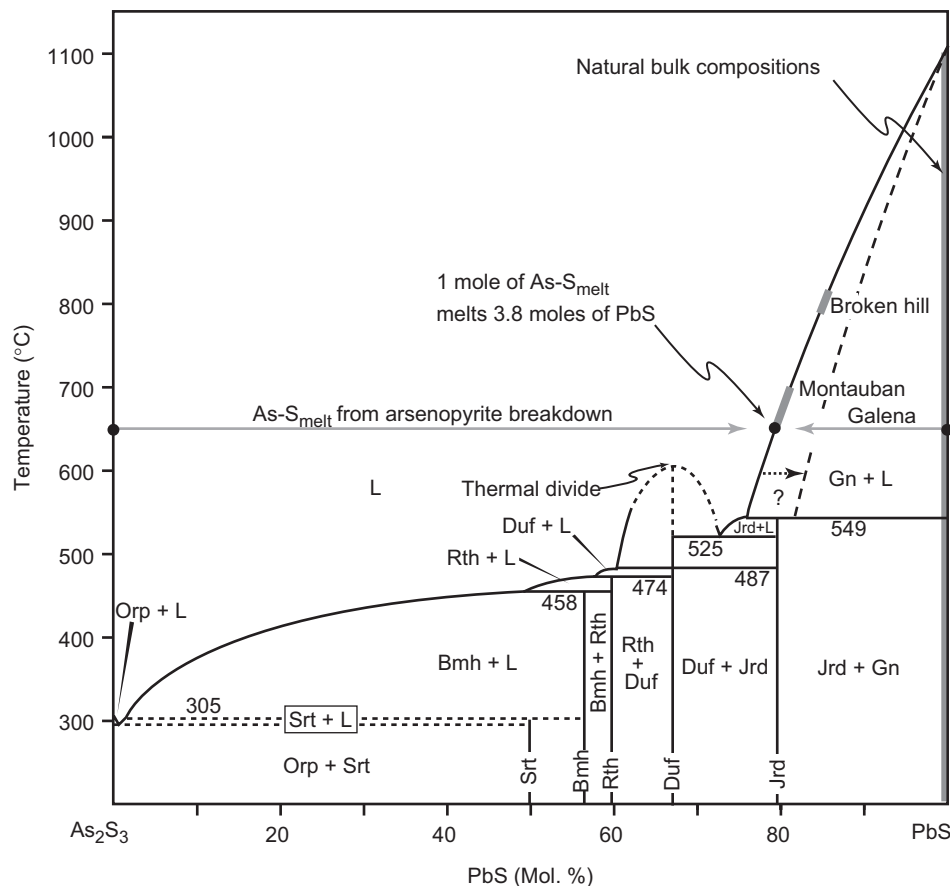
Fig. 10. As_2S_3–PbS binary phase diagram. Modified from Kutolglu (1969). The grey sections labelled Montauban and Broken Hill indicate the estimated temperatures reached during metamorphism at each locality. The narrow grey field at the right of the diagram illustrates the very small ratio of arsenopyrite to galena in mineral deposits. Dashed phase boundaries represent experimental uncertainty.

only As-bearing sulfosalts and galena, and the elements As, Pb and S. If other sulfide and sulfosalt minerals contribute to the melt, or other elements partition into the melt from unmelted sulfide minerals, then the melt ratio may actually be higher.

Once partial melting between the major sulfide minerals commences in the upper amphibolite or granulite facies (750–800°C, Table 2 and Fig. 3), the volume of melt in massive Pb–Zn sulfide deposits can substantially exceed 0·5 vol. %. The volume of melt produced at this grade of metamorphism again depends on the bulk composition. Deposits with a high proportion of galena and chalcopyrite together with some sphalerite and pyrrhotite will generate greater melt volumes than deposits containing only minor galena. Granulite-facies metamorphism of such a galena- and chalcopyrite-rich deposit could generate melt volumes in the 5–30% range, volumes that would in all probability allow segregation of sulfide magma dykes.

Our observations of crystallized sulfide melt accumulations at the Broken Hill and Montauban mines indicate significant enrichment in Sb, Ag and Bi relative to Pb, when compared with galena in the massive sulfide

units (Fig. 6). This observation is matched by that of Sparks & Mavrogenes (2005), who described similarly enriched sulfide melt inclusions at Broken Hill. Therefore, these elements, which initially would be in solid solution in galena, are interpreted to diffusively partition into As–Pb–S melts where melt communicates chemically with unmelted galena. This addition of Sb, Ag and Bi to the melt should enhance its capacity to cause further partial melting, thus causing a positive feedback effect during initial melting, although the overall effect is likely to be small because of the rarity of the elements.

Mobilization-assisted melting in massive Pb–Zn ± Cu deposits

Because the bulk compositions of massive Pb–Zn ± Cu deposits are dominated at high metamorphic grades by sphalerite, pyrrhotite, galena and in some cases chalcopyrite, the small volumes of initial melt will be saturated in most or all of these phases. Thus, extraction of a partial melt will leave some or all of these minerals in the restite. In cases where PbS is a saturated component of the partial melt, interaction between the melt and

Table 4: Arsenic contents of massive Pb–Zn ore from several deposits and calculated maximum possible percentage of As–Pb–S melt generated through arsenopyrite melting (based on whole-rock densities of 4500 kg/m^3)

Deposit/sample location	Pb (ppm)	As (ppm)	Ag (ppm)	Sb (ppm)	Bi (ppm)	Au (ppm)	Cu (%)	Zn (%)	Vol. % As–Pb–S melt at 600°C	Vol. % As–Pb–S melt at 650°C	Vol. % As–Pb–S melt at 700°C	Data source
Broken Hill (metamorphosed at ~800°C, 5 kbar; e.g. Cartwright, 1999)												
B Lode	75000	100	42	100	135				0·08	0·09	0·09	Ryall, 1979
B Lode	93000	100	50	50	150				0·08	0·09	0·09	
No. 3 lens	86000	9300	610	300	5				7·67	8·05	8·69	
No. 3 lens	96000	1800	200	300	5				1·49	1·56	1·68	
No. 3 lens	60000	1000	280	500	5				0·83	0·87	0·93	
No. 3 lens	219000	100	220	1200	5				0·08	0·90	0·09	
Mean No. 3 lens	11500	3050	328	575	5				2·52	2·64	2·85	
Dropper	267000	250	180	800	5				0·21	0·22	0·23	
Dropper	506000	450	520	800	180				0·37	0·39	0·42	
Dropper	260000	700	250	600	120				0·58	0·61	0·65	
Montauban (metamorphosed at ~650°C and 5 kbar; Bernier et al., 1987)												
MNT-001	1300	10·7	29·2	4	7	3·01	1·21	7·01	0·01	0·01	0·01	This study
MNT-002	125100	1·1	>500	234·8	1·1	0·87	0·06	21·84	0·00	0·00	0·00	
MNT-017	100	6·5	11·4	3·4	0·6	0·82	0·23	0·11	0·01	0·01	0·01	
Geco (metamorphosed at 600–700°C and 3–6 kbar; Peterson & Zaleski, 1999)												
GCO-002	3000	22·4	274·5	6·2	70·4	0·27	12·49	8·87	0·02	0·02	0·02	This study
GCO-003	161700	154·5	251·6	182·5	49·5	0·07	0·18	6·7	0·13	0·13	0·14	
GCO-006	7000	26·5	137·6	12	26·6	0	2·41	17·32	0·02	0·02	0·03	
GCO-007	1200	19·3	16·2	3·8	7·1	0·34	0·06	30·98	0·02	0·02	0·02	
GCO-011	85400	0	194·1	1·3	0	0	0·87	11·53	0·00	0·00	0·00	
GCO-018	300	117·9	17·4	2·1	1·3	0·07	1	31·21	0·10	0·10	0·11	
Calumet (metamorphosed at 650–700°C and 4–6 kbar; Williams, 1990)												
CAL-001	117300	325·2	>500	399·5	5·8	1·51	0·08	1·85	0·27	0·28	0·30	This study
CAL-009	69400	12·4	>500	355·8	13·1	0	0·03	17·73	0·01	0·01	0·01	
CAL-014	85200	43·8	479·7	390·8	4·4	0·21	0·2	24·43	0·04	0·04	0·04	
CAL-020	63700	57·1	>500	434·9	1·8	1·03	0·07	3·41	0·05	0·05	0·05	
Cannington (metamorphosed at 665–690°C and 4–6 kbar; Mark et al., 1998)												
Nithsdale	128000	540	820	730		0·06			0·45	0·47	0·50	Walters & Bailey, 1998
Cukadoo	24000	2300	82	80		0·35			1·90	1·99	2·15	
Colwell	20000	2600	84	58		0·27			2·15	2·25	2·43	
Glenholme	183000	1300	695	920		0·10			1·07	1·13	1·21	
Burnham	167000	610	820	630		0·09			0·50	0·53	0·57	
Broadlands	115000	210	430	505		0·03			0·17	0·18	0·20	

unmelted galena through mobilization-assisted melting is thought to induce preferential partitioning of Ag, Sb and Bi from unmelted galena into the melt. If this galena-saturated melt interacts with a large proportion of unmelted galena during mobilization, the melt may become extremely enriched in these elements relative to the restite. This is analogous to using R-factors to explain PGE enrichment in magmatic sulfide melts. During formation of some massive Pb–Zn ± Cu deposits, Au and Ag are preferentially precipitated together with low melting point minerals and elements (see Tormanen & Koski, 2005), increasing the likelihood that they would be incorporated into any melt produced during metamorphism, and therefore mobilized.

Evidence for preferential metal accumulation in melts

Support for the idea that initial partial melts in massive Pb–Zn deposits should be rich in As, Sb, Ag, Bi and Au (if present) and saturated in PbS, but low in Fe and Zn, is provided by the data in Fig. 7. These diagrams are a form of Harker diagram, as used by igneous petrologists to show fractionation in silicate melts, but here used to show fractionation of a sulfide melt. Figure 7 shows the approximate local bulk compositions of a number of sulfide–sulfosalt–native mineral aggregations in one small ($3 \, cm \times 2 \, cm \times 1 cm$) sample from the gold-rich part of the Montauban deposit adjacent to the massive sulfide unit (e.g. Figs. 6b and c). The abundant dyscrasite (Ag_3Sb; $T_m = 585°C$) in many of these, and pyrargyrite (Ag_3SbS_3; $T_m = 485°C$) along micro-veinlets connecting the aggregations, leaves little doubt that there was a significant proportion of sulfide melt in this sample. This is confirmed by the experiment conducted on this sample, which produced melt when subjected to P–T conditions approximating peak metamorphism (Fig. 6d).

As suggested by Fig. 10, the initial partial melt, which probably formed within the massive sulfide unit before migrating into the wall rock, was probably Pb-rich and contained significant As ($+$Sb, Ag and Au in this case). Importantly, the initial partial melt would have been saturated in galena, so when it started to cool, galena was the first mineral to crystallize. Assuming continual migration during cooling, through either gravitational or deformational processes, fractionation of the melt from the residual galena would make the melt increasingly rich in As, Sb, Ag and Au, producing the fractionation trend of Fig. 7a. The melt should be thought of as a complex many-element system, rather than as the simple binary system of Fig. 10. Thus, although there is a thermal divide in Fig. 10 that a cooling melt could encounter, the elemental complexity of the melt means that there is likely to be a series of diverging cotectics that the melt composition follows as it cools towards an ultimate eutectic. Therefore, as other sulfosalts started to crystallize with further cooling, local melt patches as well as local solid residue packets deviated in composition from the ideal fractionation line produced by galena-only crystallization. This may explain the scatter seen in Fig. 7b and c. In contrast to the bulk composition of the massive sulfide unit as a whole, which is essentially a restite, these melt accumulations contain little Fe or Zn. The Fe that is present in the accumulations may represent interaction during cooling between the Fe-poor melt and the pre-existing disseminated pyrrhotite that occurs throughout the sample. It can be seen that the initial partial melt at Montauban was enriched in Pb, As, Sb, Ag and Au, relative to the massive sulfide unit and became increasingly enriched in all but Pb as it cooled and crystallized.

Textural evidence for the existence of a sulfide melt is difficult to recognize within the massive sulfide restite at Montauban. There are no cumulate textures at this locality because only a very small proportion of the deposit melted. In any example of partial melting and melt migration within a massive Pb–Zn $\pm$ Cu deposit, the restite is likely to be relatively depleted in Pb, As, Sb, Ag, Au and possibly Cu, and enriched in Fe and Zn (Fig. 7).

Gold deposits—the influence of sulfosalts

Observations

Two gold deposits, the Challenger deposit (South Australia) and the Hemlo deposit (Ontario, Canada), have been shown to have undergone metamorphic sulfide anatexis (Tomkins & Mavrogenes, 2002; Tomkins *et al.*, 2004). The Challenger deposit, metamorphosed at granulite-facies conditions, is relatively sulfosalt-poor with a restricted ore mineral assemblage, whereas Hemlo, metamorphosed at mid-amphibolite-facies conditions (Powell *et al.*, 1999), is a sulfosalt-rich deposit with a broad array of ore minerals. Challenger probably had an assemblage typical of Archean orogenic gold mineralization (Tomkins & Mavrogenes, 2002), whereas Hemlo is thought to have had a pre-metamorphic ore mineral assemblage analogous to both epithermal and porphyry mineralization (Tomkins *et al.*, 2004).

Figure 11 shows some examples of mineral associations from each deposit that, when considered together with experimental studies, metamorphic grade and structural association, are indicative of a sulfide melt (Tomkins & Mavrogenes, 2002; Tomkins *et al.*, 2004). As in the massive Pb–Zn deposits, the examples shown in Fig. 11 are enriched in elements such as As, Sb, Bi, Au, Ag, Hg, Tl and Pb (the LMCE of Frost *et al.*, 2002), but depleted in Fe (as well as Zn and Mo at Hemlo) relative to the bulk of the sulfide material in each deposit. An additional example, from the Soimus Ilii prospect (Romania), shows that metal-rich melts can influence the distribution of gold even at comparatively low temperatures during greenschist-facies metamorphism and deformation ($>400°C$, no pressure estimate; Ciobanu *et al.*, 2006). The sulfide melt at this locality is thought to have contained Au, Bi, Pb, Te and S.

Mineralogical constraints on initial melting

Gold deposits are extremely diverse in their ore mineral associations, reflecting a wide range of formation mechanisms (Table 3). Five gold deposit types are listed in Table 3. Of these, only the alluvial gold deposits are unlikely to melt during metamorphism, simply because, in these deposits, gold is not associated with any sulfide or sulfosalt minerals that might depress the melting point of gold to lower temperatures.
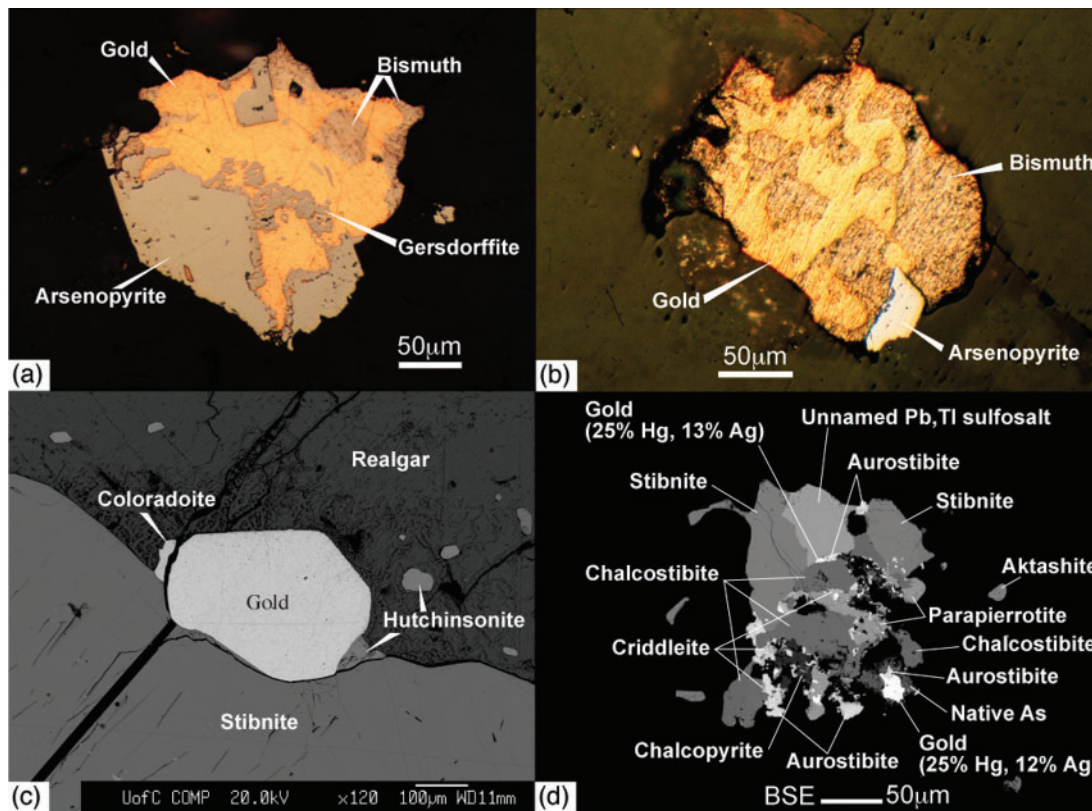
Fig. 11. Ore mineral assemblages from the Challenger and Hemlo deposits that are indicative of sulfide melting. (a, b) As in these two photomicrographs, gold invariably coexists with arsenopyrite and/or native bismuth at the Challenger deposit. (c) A BSE image of gold, coloradoite (HgTe) and hutchinsonite $[(Pb,Tl)_2(As,Sb)_5S_9]$ at the contact between stibnite and realgar in a coarse accumulation of sulfosalts between quartz boudins from the Hemlo deposit. (d) A BSE image of an aggregation of rare sulfosalts and native minerals, including gold, stibnite, native arsenic, aurostibite $(AuSb_2)$, chalcostibite $(CuSbS_2)$, aktashite $[Cu_6Hg_3(As,Sb)_4S_{12}]$, parapierrotite $[Tl(Sb,As)_5S_8]$, chalcopyrite, criddleite $(TlAg_2Au_3Sb_{10}S_{10})$ and an unnamed Pb,Tl sulfosalt, within a strongly boudinaged quartz vein from the Hemlo deposit. The unnamed Pb,Tl sulfosalt has the following composition (as measured by WDS; in wt %): Au 0, Ag 1·13, Fe 0, Cu 0·11, Zn 0·01, Hg 0·56, Pb 22·71, Tl 14·48, Sb 27·90, As 10·32, S 22·77.

The gold deposits that may start to melt during very low temperature metamorphism are those that contain sulfosalt minerals, telluride minerals, and/or native bismuth or mercury (typically epithermal deposits as well as some orogenic gold deposits). There is a diverse range of minerals and mineral systems in these deposits that can melt at low temperatures (Table 2), and many, if not all, of the resulting melts have the capacity to incorporate and mobilize gold and silver. In the example at Soimus Ilii, remobilization of Au-bearing melt commenced when native Bi melted (completely) and migrated during deformation, incorporating some Au, Pb, Te and S as it went (Ciobanu *et al.*, 2006). Most of the common sulfide minerals, including pyrite, pyrrhotite, sphalerite and chalcopyrite (as well as molybdenite), do not contribute greatly to these sulfosalt-rich low-temperature melts (Tomkins *et al.*, 2004), and therefore remain behind as residual phases during melt mobilization. This explains

the enrichment of Au and LMCE and depletion of elements such as Fe, Zn and Mo in the examples in Fig. 11. This is also essentially the same fractionation tendency as that seen in the massive Pb–Zn deposits.

Gold deposits that contain only pyrite, pyrrhotite and arsenopyrite (i.e. many orogenic Au deposits) may not start to melt during metamorphism until considerably higher temperatures are reached. Arsenopyrite + pyrite may melt at lower amphibolite-facies conditions to form As–S melt + pyrrhotite [reaction (1)], but only under high fS_2 conditions (see Tomkins *et al.*, 2006). Generation of high fS_2 conditions during metamorphism is favoured by pyrite-rich rocks that maintain moderate fO_2 (rocks that are graphite-free, for example), and that are low in Fe silicates and oxides. This is not to say that high fS_2 conditions are impossible in less favourable rocks, just that more pyrite must be consumed to generate enough sulfur to maintain equilibrium. Thus, if a deposit hosted

Table 5: Estimates of the melt percentage in metal-rich parts of the Hemlo gold deposit

Sample no.	Au (ppm)	Sb (ppm)	As (ppm)	Hg (ppm)	Pb (ppm)	Cu (ppm)	Ag (ppm)	S (wt %)	Max. melt (wt %)	Max. melt (vol. %)
440NQ-34	38·80	1100	870	83	45·1	126	2·5	4·96	0·32	0·21
440NQ-34	34·70	1500	1000	66	23·3	52	2·5	5·82	0·37	0·25
47-5W	32·10	350	340	34	23·8	68	2·5	1·6	0·12	0·08
47-5W	38·20	4500	3100	270	1·1	83	2·5	2·06	1·12	0·75
8-47	40·70	1100	27	6	9·1	36	2·5		0·17	0·10
NGG-36W	32·34	5800	670	100	37·9	80	3·0	4	0·94	0·58
NGG-36W	113·00	410	88	55	44·4	36	2·5	1·04	0·10	0·05
T-218W	78·90	2600	150	240	34·8	43	2·5	1·16	0·43	0·25
430-16	0·40	330	3800	16			2·5		0·59	0·46
9450-87-18	0·34	58	2200	5			2·5		0·32	0·25
5-13	24·80	4500	620	32			2·5		0·72	0·45

Data from Williams-Jones *et al.* (1998; an unpublished report for the Canadian Mineral Industry Research Organization). The sample numbers are as recorded by those workers. This dataset contained no information regarding whether the whole-rock samples contained structurally dilatant zones or were wholly structurally compressional zones. The sulfosalt minerals are very heterogeneously distributed at Hemlo, so this information is important.

by less favourable rocks is initially low in pyrite, all pyrite may be consumed before high fS_2 conditions are reached, precluding reaction (1) from taking place. Consequently, if the gold deposit is hosted in graphitic schist, or Fe-rich rocks such as banded iron formation or dolerite, arsenopyrite may not melt until the following reaction occurs:

$$3FeAsS\ (+Au) = 2FeS + FeAs_2 + (Au-)As - S_{melt}. \quad (8)$$
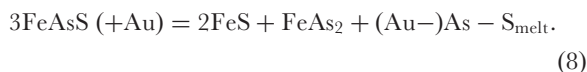
Reaction (8) proceeds at $\sim 770°C$ (at 5 kbar, $dP/dT \approx 14°C/kbar$; see Clark, 1960; Sharp *et al.*, 1985). Even these high-temperature partial melts contain little or no Fe. This reaction may also not proceed at low fS_2 conditions, as it is a desulfidation reaction and thus also governed by fS_2. It may be, therefore, that many orogenic gold deposits would not melt even at granulite-facies conditions.

Volume of melt generated

As in the massive Pb–Zn deposits, the extent of chemical communication between ore minerals in gold deposits affects melting. The disseminated nature of gold deposits means that there is little physical contact between ore minerals. However, as shown in Table 2, the many sulfosalts found in some gold deposits melt in isolation at low temperatures. Furthermore, arsenopyrite melting via reaction (1) probably does not require physical contact between arsenopyrite and pyrite. The only role of pyrite in reaction (1) is to liberate sulfur, thereby causing an increase in sulfur fugacity (Tomkins *et al.*, 2006). Therefore, if enough pyrite is breaking down in the vicinity of an

arsenopyrite crystal, a pervasive state of elevated fS_2 may be achieved, causing the arsenopyrite to melt. Once some sulfosalts have melted, mobilization caused by deformation will lead to physical interaction between melt and unmelted ore minerals, including gold, which can then be incorporated into the melt. This mobilization-assisted melting thus leads to generation of a larger proportion of melt than would otherwise be possible. However, mobilization-assisted melting may be less effective in disseminated deposits because the low melt volumes can only migrate as far as the nearest structurally dilatant domain.

Because the ore minerals in gold deposits are disseminated, the total bulk sulfide content is low, so any melt that is generated during metamorphism is likely to comprise only a small proportion of the rock volume. In this case the proportional volume of melt can be appraised by conducting bulk-rock analysis for As, Sb, Te, Tl, Pb, Cu, Hg, Bi, Au and Ag, the likely melt components, and estimating how much each element contributed to the melt (sulfur must also be taken into account). Clearly, these chemical systems can be very complex, so the result can only give a maximum (by assuming that 100% of each element contributed to the melt). In Table 5 some estimates of the melt percentage for metal-rich parts of the Hemlo gold deposit are presented. Observations of small sulfosalt accumulations that formed during mobilization of a sulfosalt melt (Tomkins *et al.* 2004) indicate that locally and at small scales the melt volume may have exceeded 25%. However, the amount of melt in the deposit as a whole would have been low (<0·5 vol. %).

Initial metamorphic melting in magmatic Ni–Cu–PGE deposits

Highly metamorphosed deposits

There have been no previous studies of Ni–Cu–PGE deposits that show that partial melting occurred during high-temperature metamorphism. However, there are at least two localities where such a possibility exists. The deposits at both localities have been metamorphosed at upper amphibolite-facies conditions and contain minerals that would melt under such conditions. These are the various deposits near Thompson in Manitoba, Canada (e.g. Peredery *et al.*, 1982), and the Las Aguilas Ni–Cu–PGE deposit in Argentina (Gervilla *et al.*, 1997). At both localities a range of rare minerals including arsenides, sulfarsenides, Pd-bismuthotellurides and antimonides have been previously interpreted to be part of a late-mobilized component of ore. At Thompson, Chen *et al.* (1993) interpreted this mobilization to be associated with late hydrothermal alteration involving conditions of 250–300°C and 3–4 kbar, whereas at Las Aguilas, Gervilla *et al.* (1997) offered no interpretation to explain the mobilization. In neither case was partial melting considered, although the mineralogy of the remobilized ore strongly suggests this as a possibility.

Constraints on initial melting

Magmatic Ni–Cu–PGE deposits form by fractionation of sulfide melt from mafic to ultramafic silicate magma (e.g. Naldrett, 1989). When this fractionation process is protracted during cooling, the sulfide melt itself evolves small amounts of lower temperature melts, which are variably enriched in As, Cu, Sb, Pb, Sn, Bi, Te, Pd, Pt, Ag and Au (Li *et al.*, 1992; Gervilla *et al.*, 1997; Pritchard *et al.*, 2004). Although the bulk of the sulfide material in these deposits typically crystallizes at temperatures beyond the realm of normal crustal metamorphism, the highly fractionated low-temperature melts may be subject to remelting, and thus mobilization, during amphibolite- to granulite-facies metamorphism.

The late fractionated component of the sulfide magma in these deposits dominantly crystallizes minerals such as arsenopyrite ($FeAsS$), gersdorffite ($NiAsS$), cobaltite ($CoAsS$), nickeline ($NiAs$), maucherite ($Ni_{11}As_8$), löllingite ($FeAs_2$), westerveldite [$(Fe,Ni)As$], safflorite [$(Co,Fe)As_2$], chalcopyrite ($CuFeS_2$) and cubanite ($CuFe_2S_3$) (Li *et al.*, 1992; Gervilla *et al.*, 1997; Pritchard *et al.*, 2004). At individual localities, this melt can be Cu-rich (e.g. Sudbury, Canada, Li *et al.*, 1992; Noril'sk, Russia, Naldrett *et al.*, 1997; Uruguayan dyke swarm, Pritchard *et al.*, 2004) or As-rich [e.g. Thompson, Canada, see Chen *et al.*, 1993; Carratraca (Spain) and Beni Bousera (Morocco) massifs, Gervilla *et al.*, 1996; Las Aguilas, Argentina, Gervilla *et al.*, 1997]. A range of rare tellurides and sulfosalts occur as minor components that crystallize from these late-stage

fractionates. Of the main minerals in As-rich and Cu-rich fractionates, only the sulfarsenides (minerals with As and S) are likely to melt under normal metamorphic conditions (Clark, 1960; Craig & Kullerud, 1967; Sharp *et al.*, 1985; Singleton & Nash, 1986; Makovicky *et al.*, 1992), although the others may melt during ultrahigh-temperature (UHT) metamorphism.

Because many of these deposits contain little or no pyrite and are dominated by pyrrhotite, pyrite decomposition during metamorphism may not buffer fS_2 to the levels required to destabilize the sulfarsenides [as in reaction (1)]. With a very high ratio of pyrrhotite to pyrite, all of the pyrite will be consumed in maintaining pyrrhotite stoichiometry, which becomes more S-rich with increasing temperature along the Py–Po buffer (Fig. 2), as well as in maintaining fluid equilibrium. In such a situation, the sulfarsenides are unlikely to melt during metamorphism through reactions that occur on the Py–Po buffer, such as reaction (1). However, mass balance calculations based on Fig. 2 suggest that as long as Po:Py <99:1 and the system is closed to external fluids, pyrite will be preserved to high enough temperatures for arsenopyrite melting to take place through reaction (1).

It is also possible that sulfarsenides in a pyrrhotite-rich massive Ni–Cu deposit could melt with increasing temperature and fS_2 through reactions within the pyrrhotite stability field, such as reaction (8) (without the Au). During metamorphism sulfur is liberated from pyrrhotite as temperature rises, leading to an increase in sulfur fugacity (Fig. 2). This desulfidation produces a steep log fS_2–T trajectory that is essentially parallel to the N_{FeS} isopleths in Fig. 2 (i.e. pyrrhotite stoichiometry stays almost the same); a trajectory that in some cases may lead to arsenopyrite melting (see Tomkins *et al.*, 2006). Cobaltite and gersdorffite may also melt by the same process, although the fS_2–T stability limits of these minerals is not known. Reaction (8) may not be applicable to other deposit types containing disseminated rather than massive pyrrhotite, as a result of processes that inhibit rising sulfur fugacity (Tomkins *et al.*, 2006).

The amount of melt that can be derived from melting of the sulfarsenides is more difficult to ascertain through a simple bulk-rock analysis, because much of the As also occurs in the arsenides (lacking S), which do not melt. However, most Ni–Cu deposits contain very small amounts of sulfarsenide minerals (e.g. Chen *et al.*, 1993), so the maximum amount of melt that can be generated from this source is probably typically less than 0·05%.

Table 2 shows the melting points of some of the rare PGE-bearing sulfosalts and bismuthotellurides that crystallize from primary late fractionated segregations. Many of these minerals start to melt at around the greenschist–amphibolite-facies transition and others melt at granulite-facies conditions or lower. Because of the

rarity of these minerals, the proportion of melt produced by their decomposition is minuscule (probably typically less than 0·01% melt). The extent to which a trace melt, incorporating Pt, Pd, Au, Ag, Bi, Te, Sb, Pb and Sn, could flux the melting of the volumetrically dominant sulfide, sulfarsenide and arsenide minerals is not well understood. Makovicky *et al.* (1992) showed that at 850°C in the system Pt–Fe–As–S, two relevant Pt-bearing melts exist; a Pt–As melt with 28–39 at. % As and a Fe–As–Pt melt with up to 23·7 at. % Pt, 31·7 at. % As and 2·6 at. % S. Thus, a complex PGE-bearing bismuthotelluride–sulfosalt melt could cause some (very minor) partial melting of the main phases at metamorphic conditions experienced in the crust.

Disseminated Cu deposits (porphyry/IOCG/redbed/skarn)

These genetically differdnt types of deposits have been grouped in this section because (1) they each contain sulfide mineral assemblages that are dominated by iron sulfides and copper–iron sulfides, and (2) it is the sulfide bulk composition that has the most important influence on the initiation of melting. Skarn deposits are a special case in that as a group they have highly varied ore mineralogies. Although economically exploitable skarn deposits may be mined for W, Sn, Mo, Cu, Fe, Pb–Zn or Au, we have included them in this category because several of the world's largest porphyry Cu deposits also have Cu–Au skarns associated with them, whereas Zn–Pb and Au-only skarns are economically less significant. The discussion developed in previous sections applies also to melting of Zn–Pb or Au-only skarns. In particular, Au-only skarns often have native Bi and sulfosalt-rich assemblages that are highly susceptible to melting during metamorphism.

Examples of amphibolite- and granulite-hosted Cu deposits

Few examples exist of Cu deposits metamorphosed at conditions beyond mid-amphibolite facies. Although the deposits at Okiep in South Africa do not conform to one of the categories identified in the title of this section, they deserve special mention. These deposits are likely to be associated with mafic magmatism and have abnormally Cu-rich sulfide mineral assemblages that are dominated by bornite and chalcopyrite (Maier, 2000). This assemblage makes them distinct from other magmatic Ni–Cu–PGE deposits, which are typically pyrrhotite- and pentlandite-rich. These deposits were metamorphosed at conditions of approximately 750–820°C and 5–6 kbar (Raith & Harley, 1998). Similar deposits occur in the Curaca Valley, Brazil, which also have an unusually high proportion of bornite and chalcopyrite and may have been metamorphosed at granulite-facies conditions (Maier & Barnes, 1999). As will be discussed below, the sulfide mineral assemblages at the Okiep and Curaca Valley deposits may start to melt at these metamorphic grades, but the possibility of partial metamorphic sulfide anatexis has not yet been investigated.

Constraints on melting

In general, when disseminated copper deposits first form, the ore mineral assemblage is typically dominated by pyrite and chalcopyrite, and may contain appreciable amounts of bornite and molybdenite. Many minor sulfide minerals may also occur, particularly in some skarn deposits, including a range of Cu-sulfides, galena, sphalerite, gold, bismuth minerals (including native bismuth), tellurides and sulfosalts (particularly tetrahedrite–tennantite). Except in some skarn deposits, the sulfide minerals are disseminated, and in most deposits comprise only a small proportion of the bulk rock.

Ore minerals that melt at low temperatures (sulfosalts, tellurides and native Bi) tend to occur in Au-rich, Cu-poor varieties of these deposits. Examples include the Lucky Draw deposit in Australia (a Au–Bi–Te skarn; Sheppard *et al.*, 1995) and the Nico prospect in northern Canada (a Co–Au–Bi Fe-oxide deposit; Goad *et al.*, 2000). The melting relationships in the sulfosalt- and telluride-rich deposits have been described in the section on gold deposits. In deposits that lack sulfosalt minerals, telluride minerals and/or native Bi, partial melting may not commence until much higher temperatures are reached. During metamorphism copper sulfides, such as chalcocite (Cu_2S) and covellite (CuS), react with the typically coexisting pyrite to produce Cu–Fe-sulfide solid solutions [bornite$_{ss}$ and intermediate solid solution (ISS)] and pyrrhotite$_{ss}$ (Yund & Kullerud, 1966). In the absence of other phases, these assemblages will not start to melt until high temperatures consistent with the granulite facies are reached (slightly less than 800°C at 1 bar; Tsujimura & Kitakaze, 2004), when bornite$_{ss}$ + ISS or bornite + pyrrhotite$_{ss}$ break down incongruently to produce a Cu–Fe–S melt. Many copper deposits contain these assemblages (including the deposits at Okiep, South Africa, and the Curaca Valley, Brazil) and it can be seen from published ore grades that melt proportions exceeding 0·5 vol. % could conceivably be generated through high-temperature metamorphism. Again, the disseminated nature of the mineralization in these deposits means that mineral communication would limit the proportion of melt produced (mobilization-assisted melting is less effective in disseminated deposits).

Molybdenite, if present, may react with coexisting pyrite to produce a Mo–Fe–S melt at ~735°C (at 1 bar; Grover *et al.*, 1975), but this reaction can only proceed under the very high fS_2 conditions required for pyrite to exist at this temperature. Preservation of pyrite to such a high temperature requires moderately oxidized host rocks that are low in Fe silicates and oxides, and that little hydrothermal fluid is generated by breakdown of phyllosilicates.

Thus, partial melting of molybdenite + pyrite may be possible in parts of porphyry Cu deposits that are low in phyllosilicates, and some skarn deposits (molybdenite does not typically occur in iron-oxide copper gold (IOCG) or sediment-hosted stratiform Cu deposits). However, unlike reaction (1) where pyrite is simply required to raise $f S_2$ and thus need not be in immediate contact with arsenopyrite, partial melting between molybdenite and pyrite incorporates a considerable proportion of Fe into the melt. Therefore, pyrite and molybdenite need to be in physical contact for partial melting to proceed, a requirement that is not ubiquitously met because of the disseminated nature of these minerals in porphyry deposits and also skarn deposits. Even if pyrite did survive to high temperatures, the low proportion of molybdenite in these deposits (average grades as high as 0·45% MoS_2 are recorded in some deposits, but 0·1% is more typical; Carten *et al.*, 1993) and the poor chemical communication between the minerals implies that the volume of melt that can be generated through this reaction is likely to be low (less than 0·1%). An interesting complication in a metamorphosed ıporphyry system is that the hydrothermally altered silicate host rock would start to melt before the sulfide minerals, therefore mobilization of silicate melt could promote mobilization of even trace quantities of sulfide melt (Tomkins & Mavrogenes, 2002, 2003).

The system Cu–Mo–Fe–S has not been studied by experimentalists. However, Grover & Moh (1969) found that in the system Cu–Mo–S, molybdenite and chalcocite coexist without melting at 800°C and melt only in the presence of excess sulfur at 1000°C. These data suggest that the presence of molybdenite may not greatly affect the temperature of the melting reactions in the system Cu–Fe–S, described above. Based on these arguments we suggest that disseminated Cu deposits that lack bornite at peak metamorphic conditions are unlikely to produce >0·5 vol. % melt within the limits of typical crustal metamorphism (including those that contain sulfosalts), whereas bornite-bearing deposits may be capable of generating >0·5 vol. % melt at granulite-facies conditions. UHT metamorphism would be capable of generating a significant proportion of sulfide melt in many Cu deposits.

MOBILIZATION OF POLYMETALLIC MELT AT LOW MELT FRACTIONS

We have shown that the amount of melt that can be generated by melting of sulfosalt minerals at greenschist- or amphibolite-facies conditions in ore deposits is either very small or non-existent. Theoretical and experimental studies both suggest that texturally equilibrated mineral–melt systems (which are expected at amphibolite-facies conditions) are permeable with melt proportions as low as

0·5 vol. %, where the wetting angle is less than 60° (Cheadle *et al.*, 2004). Therefore, in gold deposits, magmatic Ni–Cu–PGE deposits and bornite-poor disseminated Cu deposits the proportion of melt that can be generated during even granulite-facies metamorphism may typically be too small for any migration to occur without significant deformation.

However, in some deposits such as Hemlo, there is strong structural and geochemical evidence of significant melt migration despite low melt percentages. At Hemlo, melt accumulated in structurally dilatant domains and is highly enriched in gold and other elements; the metal enrichment suggests that some material was incorporated as the melt migrated (Tomkins *et al.*, 2004). This migration, driven by intense ductile deformation that bracketed peak metamorphism, appears to have been restricted to distances on the scale of centimetres to meters as a result of an abundance of dilational features, such as boudin necks between extended feldspathic layers and quartz veins. Although the length scale of migration is difficult to constrain, evidence for through-going sulfide melt migration has not been found at Hemlo. This is because melts cannot migrate beyond dilational zones until the structures are volumetrically overwhelmed.

However, if higher melt proportions, >0·5 vol. %, are generated, for example during high-temperature metamorphism of a massive Pb–Zn(–Cu) deposit in which major phase sulfide minerals become involved in partial melting, migration may occur in the absence of deformation, through gravitational segregation. The feasibility of this gravitational segregation depends upon the wetting properties of sulfide melts interacting with unmelted sulfide minerals and with silicates, which are largely unknown. However, low interfacial angles (<60°) between galena and sphalerite in massive sulfide units at Broken Hill have been interpreted by Frost *et al.* (2002) to reflect crystallization of a galena-rich partial melt that wetted residual sphalerite. In addition, our observations suggest that interfacial angles between sulfide or sulfosalt melt and solid silicates at least in some cases are less than 60° (Fig. 12), suggesting that gravitational migration is possible in the absence of deformation, and where the melt proportion is in excess of 0·5%. This migration would be in the downward direction because of the relative densities of the melt and restite. It is possible that the rock may become permeable enough to transmit smaller quantities of sulfide melt if a, mostly immiscible, hydrothermal fluid is present to enhance porosity.

DISCUSSION AND CONCLUSIONS

The most important factor governing initiation of melting in a metamorphosed ore deposit is the composition of the original mineral assemblage. A deposit of any type with a significant proportion of sulfosalts is capable of
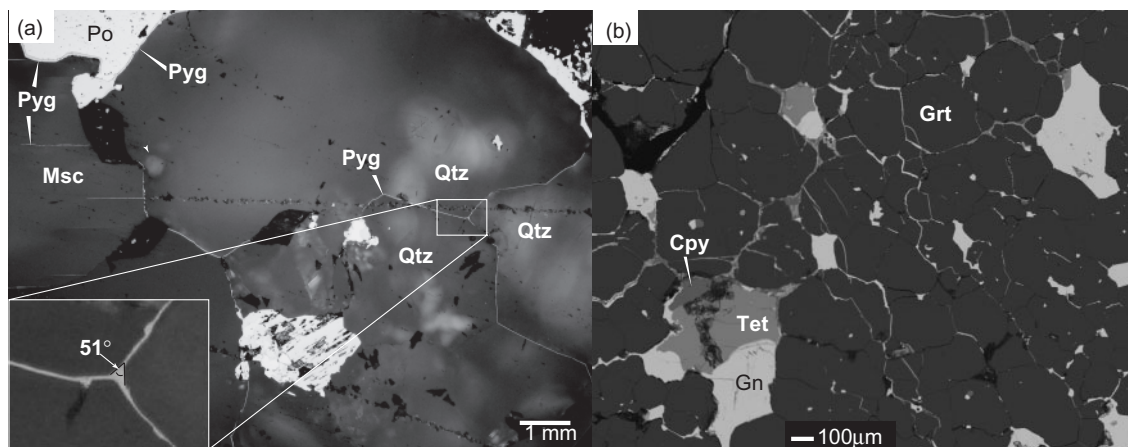
Fig. 12. Microveinlet arrays of sulfide melt between silicate grains. (a) Photomicrograph of pyrargyrite (Pyg; $T_m \sim 485°C$) microveinlets along quartz (Qtz) grain boundaries and muscovite (Msc) cleavage and enveloping pyrrhotite (Po) from the Montauban deposit. (b) BSE image of extensive microveinlet arrays involving galena (Gn), Ag-tetrahedrite (Tet) and chalcopyrite (Cpy) along garnet (Grt) grain boundaries from the Broken Hill deposit.

generating some melt within the greenschist or amphibolite facies. In contrast, sulfide deposits lacking sulfosalts or tellurides may not start to melt until the upper amphibolite or granulite facies, if at all (Fig. 3). Deposits that most typically have appropriate mineral assemblages for low-temperature partial melting are sulfosalt-rich epithermal gold deposits. Massive Pb–Zn deposits, typically being galena-rich and containing minor arsenopyrite, may start to melt in the middle to upper amphibolite facies. Although bornite-bearing disseminated Cu deposits may start to melt at granulite-facies conditions, those deficient in bornite and sulfosalts may not melt during typical crustal metamorphism (UHT metamorphism is regarded as atypical). The most highly fractionated, As-rich parts of some magmatic Ni deposits may produce a very small proportion of melt within the limits of typical metamorphism, whereas Ni deposits lacking such features cannot remelt.

Although many types of sulfosalt-bearing gold deposits are capable of partially melting at greenschist- or amphibolite-facies conditions, large volumes of melt are unlikely to accumulate through mobilization. This is because the minerals in gold deposits that melt are invariably sparsely disseminated and the total volume of melt, when the deposit is considered as a whole, is relatively small. In addition, in deformed deposits the silicate host rock typically develops a dispersed array of micro- to meso-scale dilational structures during deformation, into which local aliquots of melt would migrate and then remain, thus precluding accumulation into through-going veins and dykes that drain the rock. In this way accumulation of large volumes of sulfide melt may also be prevented from forming in bornite-rich disseminated Cu deposits, despite their potential for forming melt volumes

exceeding 0·5%. Volumes of sulfide melt significant enough to coalesce into larger bodies of magma capable of being mobilized distances of hundreds of meters to kilometers are most likely in highly metamorphosed massive Pb–Zn–Cu deposits. This conclusion is reached for three reasons: (1) massive sulfide deposits are likely to contain enough sulfide material to form significantly more than 0·5 vol. % melt; (2) the eutectic between common sulfide minerals is lowest in systems that contain galena + chalcopyrite; (3), fewer meso- to microscale dilational structures form within massive sulfide assemblages during deformation. Where galena forms a significant proportion of a sulfide assemblage that also contains chalcopyrite, larger bodies of sulfide magma are likely to form from massive Pb–Zn–Cu deposits as the metamorphic temperature exceeds about 700–730°C (at 2 kbar), particularly if deformation is active at these conditions.

Once these larger volumes of sulfide magma start to form into dykes, outliers of mineralization could start to form at significant distances from the source ore body. Theoretically, in granulite terrains this process could lead to formation of small new satellite ore bodies around a source deposit. Once these outliers are identified as sulfide magma dykes sourced from elsewhere, they can potentially be traced by explorationists to the source if it remains unidentified. However, excepting the mechanism suggested by Tomkins & Mavrogenes (2003), where sparse amounts of sulfide melt segregate in concert with migmatitic silicate melt to form metal-rich magma, completely new ore bodies are unlikely to form through melting of dispersed sulfide material that was not previously economic. Nevertheless, native metal melts and possibly sulfosalt melts may play a role in localization of gold in particular during formation

of several different types of ore deposits. Douglas *et al.* (2000) suggested that native Bi may be precipitated as a liquid from hydrothermal fluids (Bi has a melting point of 271·4°C; Fig. 1) and that it may then scavenge Au from solution. Many have noticed a close association between Au and Bi in a range of deposit types (e.g. Ciobanu *et al.*, 2006), and it has been proposed that the Douglas model is responsible for Au precipitation at an actively forming mineralization center in the Escabana Trough, east Pacific Ocean (Tormanen & Koski, 2005). It is possible that native mercury and sulfosalts with low melting temperatures have played a similar role at other localities.

ACKNOWLEDGEMENTS

REFERENCES

Baile, R. H. & Reid, D. L. (2005). Ore textures and possible sulfide partial melting at Broken Hill, Aggenys, South Africa I: Petrography. *South African Journal of Geology* **108**, 51–70.

Barton, P. B., Jr (1969). Thermochemical study of the system Fe–As–S. *Geochimica et Cosmochimica Acta* **33**, 841–857.

Barton, P. B., Jr (1971). The Fe–Sb–S system. *Economic Geology* **66**, 121–132.

Bernier, L., Pouliot, G. & MacLean, W. H. (1987). Geology and metamorphism of the North Montauban Gold Zone: a metamorphosed polymetallic exhalative deposit, Grenville Province, Quebec. *Economic Geology* **82**, 2076–2090.

Blackburn, W. H. & Schwendeman, J. F. (1977). Trace-element substitution in galena. *Canadian Mineralogist* **15**, 365–373.

Boyd, F. R. & England, J. L. (1960). Apparatus for phase-equilibrium measurements at pressures up to 50 kilobars and temperatures up to 1750°C. *Journal of Geophysical Research* **65**, 741–748.

Brett, R. & Bell, P. M. (1969). Melting relations in the Fe-rich portion of the system Fe–FeS at 30 kb pressure. *Earth and Planetary Science Letters* **6**, 479–482.

Brett, R. & Kullerud, G. (1967). The Fe–Pb-S system. *Economic Geology* **62**, 354–369.

Bryndzia, L. T. & Davis, A. M. (1989). Liquidus phase relations on the quasi-binary join Cu$_2$S–Sb$_2$S$_3$: Implications for the formation of tetrahedrite and skinnerite. *American Mineralogist* **74**, 236–242.

Bryndzia, L. T. & Kleppa, O. J. (1988). High-temperature reaction calorimetry of solid and liquid phases in the quasi-binary system Ag$_2$S–Sb$_2$S$_3$. *Geochimica et Cosmochimica Acta* **52**, 167–176.

Cabri, L. J. (1965). Phase relations in the Au–Ag–Te system and their mineralogical significance. *Economic Geology* **60**, 1569–1606.

Cabri, L. J., Harris, D. C. & Gait, R. I. (1973). Michenerite (PdBiTe) redefined and froodite (PdBi$_2$) confirmed from the Sudbury area. *Canadian Mineralogist* **11**, 903–912.

Carten, R. B., White, W. H. & Stein, H. J. (1993). High-grade granite-related porphyry molybdenum systems: classification and origin. In: Kirkham, R. V., Sinclair, W. D., Thorpe, R. I. & Duke, J. M. (eds) *Mineral Deposit Modeling. Geological Association of Canada, Special Paper* **40**, 521–554.

Cartwright, I. (1999). Regional oxygen isotope variation at Broken Hill, New South Wales, Australia: large-scale fluid flow and implications for Pb–Zn–Ag mineralization. *Economic Geology* **94**, 357–373.

Chang, L. L. Y. & Knowles, C. R. (1977). Phase relations in the systems PbS–Fe$_{1−x}$S–Sb$_2$S$_3$ and PbS–Fe$_{1−x}$S–Bi$_2$S$_3$. *Canadian Mineralogist* **15**, 374–379.

Cheadle, M. J., Elliot, M. T. & McKenzie, D. (2004). Percolation threshold and permeability of crystallizing igneous rocks: the importance of textural equilibrium. *Geology* **32**, 757–760.

Chen, Y., Fleet, M. E. & Pan, Y. (1993). Platinum-group minerals and gold in arsenic-rich ore at the Thompson mine, Thompson Nickel Belt, Manitoba, Canada. *Mineralogy and Petrology* **49**, 127–146.

Ciobanu, C. L., Cook, N. J., Damian, F. & Damian, G. (2006). Gold scavenged by bismuth melts: an example from alpine shear-remobilizates in the Highis Massif, Romania. *Mineralogy and Petrology* **87**, 351–384.

Clark, L. A. (1960). The Fe–As–S system: phase relations and applications. *Economic Geology* **55**, 1345–1381 (Part I).

Connolly, J. A. D. & Cesare, B. (1993). C–O–H–S fluid composition and oxygen fugacity in graphitic metapelites. *Journal of Metamorphic Geology* **11**, 379–388.

Craig, J. R. & Kullerud, G. (1967). The Cu–Fe–Pb–S system. *Carnegie Institution of Washington Yearbook* **65**, 344–352.

Craig, J. R. & Vokes, F. M. (1993). The metamorphism of pyrite and pyritic ores: an overview. *Mineralogical Magazine* **57**, 3–18.

Dobson, D. P., Crichton, W. A., Vocaldo, L., Jones, A. P., Wang, Y., Uchida, T., Rivers, M., Sutton, S. & Brodholt, J. P. (2000). *In situ* measurement of viscosity of liquids in the Fe–FeS system at high pressures and temperatures. *American Mineralogist* **85**, 1838–1842.

Douglas, N., Mavrogenes, J., Hack, A. & England, R. (2000). The liquid bismuth collector model: an alternative gold deposition mechanism. In: Skilbeck, C. G. & Hubble, T. C. T. (eds) *Understanding planet Earth; searching for a sustainable future; on the starting blocks of the third millennium. Geological Society of Australia, 15th Australian Geological Convention, Sydney, Abstracts*. Sydney: Geological Society of Australia, 135 pp.

Elliot, R. P. (1965). *Constitution of Binary Alloys, First Supplement*. New York: McGraw–Hill.

Freidrich, K. (1907). The binary systems FeS–ZnS and FeS–PbS. *Metallurgie* **4**, 479–485 (in German).

Frost, B. R., Mavrogenes, J. A. & Tomkins, A. G. (2002). Partial melting of sulfide ore deposits during medium- and high-grade metamorphism. *Canadian Mineralogist* **40**, 1–18.

Frost, B. R., Swapp, S. M. & Gregory, R. W. (2005). Prolonged existence of sulfide melt in the Broken Hill orebody, New South Wales, Australia. *Canadian Mineralogist* **43**, 479–493.

Gervilla, F., Leblanc, M., Torres-Ruiz, J. & Hach-Ali, P. F. (1996). Immiscibility between arsenide and sulfide melts: a mechanism for the concentration of noble metals. *Canadian Mineralogist* **34**, 485–502.

Gervilla, F., Sanchez-Anguita, A., Acevedo, R. D. & Hach-Ali, P. F. (1997). Platinum-group element sulpharsenides and Pd bismuthotellurides in the metamorphosed Ni–Cu deposit at Las Aguilas (province of San Luis, Argentina). *Mineralogical Magazine* **61**, 861–877.

Goad, R. E., Mumin, A. H., Duke, N. A., Neale, K. L., Mulligan, D. L. & Camier, W. J. (2000). The NICO and Sue-Dianne Proterozoic, iron oxide-hosted, polymetallic deposits, Northwest Territories; application of the Olympic Dam model in exploration. *Exploration and Mining Geology* **9**, 123–140.

Grover, B. & Moh, G. H. (1969). Phasengleichgewichtsbeziehungen im System Cu–Mo–S in Relation zu natuerlichen Mineralien (Phase equilibria relations in the Cu–Mo–S system with reference to natural minerals.). *Neues Jahrbuch für Mineralogie, Monatshefte* **12**, 529–544.

Grover, B., Kullerud, G. & Moh, G. H. (1975). Phase equilibrium conditions in the ternary Fe–Mo–S system in relation to natural minerals and ore deposits. *Neues Jahrbuch für Mineralogie, Abhandlungen* **124**, 246–272.

Hansen, M. & Aderko, K. (1958). *Constitution of Binary Alloys*. New York: McGraw–Hill, 1305 pp.

Hoda, S. N. & Chang, L. L. Y. (1975). Phase relations in the systems PbS–Ag$_2$S–Sb$_2$S$_3$ and PbS–Ag$_2$S–Bi$_2$S$_3$. *American Mineralogist* **60**, 621–633.

Hofmann, B. A. (1994). Formation of a sulfide melt during alpine metamorphism of the Lengenbach polymetallic sulfide mineralization, Bintal, Switzerland. *Mineralium Deposita* **29**, 439–442.

Hofmann, B. A. & Knill, M. D. (1996). Geochemistry and genesis of the Lengenbach Pb–Zn–As–Tl–Ba-mineralisation, Binn Valley, Switzerland. *Mineralium Deposita* **31**, 319–339.

Knill, M. D. (1996). The Pb–Zn–As–Tl–Ba deposit at Legenbach, Binn valley, Switzerland. *Geotechnische Serie, Schweizerische Geotechnische Kommission* **90**, 74 pp.

Kojima, S. & Sugaki, A. (1984). Phase relations in the central portion of the Cu–Fe–Zn–S system between 800°C and 500°C. *Mineralogical Journal* **12**, 15–28.

Kutolglu, A. (1969). Rotogenographische und thermische Untersuchungen im quasibinaren System PbS–As$_2$S$_3$. *Neues Jahrbuch für Mineralogie. Monatshefte* **2**, 68–72.

Lawrence, L. J. (1967). Sulfide neomagmas in highly metamorphosed sulfide ore deposits. *Mineralium Deposita* **2**, 5–10.

Li, C., Naldrett, A. J., Coats, C. J. A. & Johannessen, P. (1992). Platinum, palladium, gold, and copper-rich stringers at the Strathcona mine, Sudbury: their enrichment by fractionation of a sulfide liquid. *Economic Geology* **87**, 1584–1598.

Liu, L.-G. & Bassett, W. A. (1986). *Elements, Oxides and Silicates. High-pressure Phases with Implications for the Earth's Interior*. New York: Oxford University Press, 250 pp.

Maier, W. D. (2000). Platinum-group elements in Cu-sulfide ores at Carolusberg and East Okiep, Namaqualand, South Africa. *Mineralium Deposita* **35**, 422–429.

Maier, W. D. & Barnes, S.-J. (1999). The origin of Cu sulfide deposits in the Curaca Valley, Bahia, Brazil: evidence from Cu, Ni, Se and platinum-group element concentrations. *Economic Geology* **94**, 165–183.

Makovicky, M., Makovicky, E. & Rose-Hansen, J. (1992). The phase system Pt–Fe–As–S at 850°C and 470°C. *Neues Jahrbuch für Mineralogie, Monatshefte* **10**, 441–453.

Mark, G., Phillips, G. N. & Pollard, P. J. (1998). Highly selective partial melting of pelitic gneiss in Cannington, Cloncurry district, Queensland. *Australian Journal of Earth Sciences* **45**, 169–176.

Marshall, B., Vokes, F. M., & Larocque, A. C. L. (2000). Regional metamorphic remobilisation: upgrading and formation of ore deposits. In: Spry, P. G., Marshall, B. & Vokes, F. M. (eds) *Metamorphosed and Metamorphogenic Ore Deposits. Reviews in Economic Geology* **16**, 19–38.

Maske, S. & Skinner, B. J. (1971). Studies of the sulfosalts of copper I. Phases and phase relations in the system Cu–As–S. *Economic Geology* **66**, 901–918.

Massalski, T. B., Okamoto, H., Subramanian, P. R. & Kacprzak, L. (eds) (1990). *Binary Alloy Phase Diagrams*, 2nd edn. Metals Park, OH: American Society for Metals.

Mavrogenes, J. A., MacIntosh, I. W. & Ellis, D. J. (2001). Partial melting of the Broken Hill galena–sphalerite ore—experimental studies in the system PbS–FeS–ZnS–(Ag$_2$S). *Economic Geology* **96**, 205–210.

Medvedeva, Z. S., Klochko, M. A., Kuznetsov, V. G. & Andreeva, S. N. (1961). Structural diagram of the Pd–Te alloy system. *Zhurnal Neorganicheskoi Khimii* **6**, 1737–1739.

Mungall, J. E. & Brenan, J. M. (2003). Experimental evidence for the chalcophile behavior of the halogens. *Canadian Mineralogist* **41**, 207–220.

Naldrett, A. J. (1989). *Magmatic Sulfide Deposits. Oxford Monographs on Geology and Geophysics, 14*. New York: Clarendon Press, 186 pp.

Naldrett, A. J., Ebel, D. S., Mohammed, A., Morrison, G. & Moore, C. M. (1997). Fractional crystallisation of sulfide melts as illustrated at Noril'sk and Sudbury. *European Journal of Mineralogy* **9**, 365–377.

Okamoto, H. & Massalski, T. B. (1986a). Au–Bi (gold–bismuth). In: Massalski, T. B., Murray, J. L., Bennet, L. H. & Baker, H. (eds) *Binary Alloy Phase Diagrams, 1*. Metals Park, OH: American Society for Metals, pp. 238–240.

Okamoto, H. & Massalski, T. B. (1986b). Au–Sb (gold–antimony). In: Massalski, T. B., Murray, J. L., Bennet, L. H. & Baker, H. (eds) *Binary Alloy Phase Diagrams, 1*. Metals Park, OH: American Society for Metals pp. 305 and 308–309.

Okamoto, H. & Massalski, T. B. (1986c). Au–Te (gold–tellurium). In: Massalski, T. B., Murray, J. L., Bennet, L. H. & Baker, H. (eds) *Binary Alloy Phase Diagrams, 1*. Metals Park, OH: American Society for Metals, pp. 322–323.

Okamoto, H. & Massalski, T. B. (1986d). Au–Hg (gold–mercury). In: Massalski, T. B., Murray, J. L., Bennet, L. H. & Baker, H. (eds) *Binary Alloy Phase Diagrams,1*. Metals Park, OH: American Society for Metals pp. 265 and 267.

Osadchii, E. G. (1990). The kesterite–velikite (Cu$_2$Zn$_{1-x}$Hg$_x$SnS$_4$) and sphalerite–metacinnabarite (Zn$_{1-x}$Hg$_x$S) solid solutions in the system Cu$_2$SnS$_3$–Zn–HgS at temperatures of 850, 700 and 550°C. *Neues Jahrbuch für Mineralogie, Monatshefte* **H1**, 13–34.

Pattison, D. R. M. (1992). Stability of andalusite and sillimanite and the Al$_2$SiO$_5$ triple point; constraints from the Ballachulish aureole, Scotland. *Journal of Geology* **100**, 423–446.

Pattison, D. R. M., Chacko, T., Farquhar, J. & McFarlane, C. R. M. (2003). Temperatures of granulite-facies metamorphism; constraints from experimental phase equilibria and thermobarometry corrected for retrograde exchange. *Journal of Petrology* **44**, 867–900.

Peredery, W. V., & Geological Staff (1982). Geology and nickel sulfide deposits of the Thompson Belt, Manitoba. In: Hutchinson, R. W., Spence, C. D. & Franklin, J. M. (eds) *Precambrian Sulfide Deposits. Geological Association of Canada, Special Paper* **25**, 165–209.

Peterson, V. L. & Zaleski, E. (1999). Structural history of the Manitouwadge greenstone belt and its volcanogenic Cu–Zn massive sulfide deposits, Wawa subprovince, south–central Superior Province. *Canadian Journal of Earth Sciences* **36**, 606–625.

Phillips, G. N. (1980). Water activity changes across an amphibolite–granulite facies transition, Broken Hill, Australia. *Contributions to Mineralogy and Petrology* **75**, 377–386.

Plimer, I. M. (1987). Remobilisation in high grade metamorphic environments. *Ore Geology Reviews* **2**, 231–245.

Powell, W. G., Pattison, D. R. M. & Johnston, P. (1999). Metamorphic history of the Hemlo gold deposit from Al_2SiO_5 mineral assemblages, with implications for the timing of mineralization. *Canadian Journal of Earth Sciences* **36**, 33–46.

Prince, A., Raynor, G. V. & Evans, D. S. (1990). *Phase Diagrams of Ternary Gold Alloys*. London: Institute of Metals.

Pritchard, H. M., Hutchison, D. & Fisher, P. C. (2004). Petrology and crystallization history of multiphase sulfide droplets in a mafic dike from Uraguay: implications for the origin of Cu–Ni–PGE sulfide deposits. *Economic Geology* **99**, 365–376.

Raith, J. G. & Harley, S. L. (1998). Low-P/high-T metamorphism in the Okiep Copper District, western Namaqualand, South Africa. *Journal of Metamorphic Geology* **16**, 281–305.

Roland, G. W. (1968). The system Pb–As–S. *Mineralium Deposita* **3**, 249–260.

Ryall, W. R. (1979). Mercury in the Broken Hill (N.S.W., Australia) lead–zinc–silver lodes. *Journal of Geochemical Exploration* **11**, 175–194.

Ryzhenco, B. & Kennedy, G. C. (1973). The effect of pressure on the eutectic of the system Fe–FeS. *American Journal of Science* **273**, 803–810.

Salanci, B. (1979). Contribution to the system PbS–Sb_2S_3 in relation to lead–antimony-sulfosalts. *Neues Jahrbuch für Mineralogie, Abhandlungen* **135**, 315–326 (in German).

Sharp, Z. D., Essene, E. J. & Kelly, W. C. (1985). A re-examination of the arsenopyrite geothermometer: pressure considerations and applications to natural assemblages. *Canadian Mineralogist* **23**, 517–534.

Sheppard, S., Walshe, J. L. & Pooley, G. D. (1995). Noncarbonate, skarnlike Au–Bi–Te mineralization, Lucky Draw, New South Wales, Australia. *Economic Geology* **90**, 1553–1569.

Singleton, M. & Nash, P. (1986). As–Ni (arsenic–nickel). In: Massalski, T. B., Murray, J. L., Bennet, L. H. & Baker, H. (eds) *Binary Alloy Phase Diagrams,1*. Metals Park, OH: American Society for Metals, 214 pp.

Skinner, B. & Johnson, C. (1987). Evidence for movement of ore materials during high grade metamorphism. *Ore Geology Reviews* **2**, 191–204.

Sobott, R. J. G. (1984). Sulfosalts and Tl_2S–As_2S_3–Sb_2S_3–S phase relations. *Neues Jahrbuch für Mineralogie, Abhandlungen* **150**, 54–59.

Sparks, H. A. & Mavrogenes, J. A. (2005). Sulfide melt inclusions as evidence for the existence of a sulfide partial melt at Broken Hill, Australia. *Economic Geology* **100**, 773–779.

Spear, F. S. (1993). *Metamorphic Phase Equilibria and Pressure–Temperature–Time Paths* Mineralogical Society of America Monograph, 799 pp.

Springer, G. & Laflamme, J. H. (1971). The system Bi_2S_3–Sb_2S_3. *Canadian Mineralogist* **10**, 847–853.

Stamatelopoulou-Seymour, K. & MacLean, W. H. (1984). Metamorphosed volcanogenic ores at Montauban, Grenville Province, Quebec. *Canadian Mineralogist* **22**, 595–604.

Stevens, B. P. J., Barnes, R. G., Brown, R. E., Stroud, W. J. & Willis, I. L. (1988). The Willyama Supergroup in the Broken Hill and Euriowie blocks, New South Wales. *Precambrian Research* **40–41**, 297–327.

Stevens, G., Prinz, S. & Rozendaal, A. (2005). Partial melting of the assemblage sphalerite + galena + pyrrhotite + chalcopyrite + sulfur: implications for high-grade metamorphosed massive sulfide deposits. *Economic Geology* **100**, 781–786.

Tomkins, A. G. & Mavrogenes, J. A. (2002). Mobilization of gold as a polymetallic melt during pelite anatexis at the Challenger gold deposit, South Australia: a metamorphosed Archean deposit. *Economic Geology* **97**, 1249–1271.

Tomkins, A. G. & Mavrogenes, J. A. (2003). Generation of metal-rich felsic magmas during crustal anatexis. *Geology* **31**, 765–768.

Tomkins, A. G., Pattison, D. R. M. & Zaleski, E. (2004). The Hemlo gold deposit, Ontario: an example of melting and mobilization of a precious metal–sulfosalt assemblage during amphibolite facies metamorphism and deformation. *Economic Geology* **99**, 1063–1084.

Tomkins, A. G., Frost, B. R. & Pattison, D. R. M. (2006). Arsenopyrite melting during metamorphism of sulfide ore deposits. *Canadian Mineralogist* **44**, 1325–1342.

Tormanen, T. O. & Koski, R. (2005). Gold enrichment and the Bi–Au association in pyrrhotite-rich massive sulfide deposits, Escabana Trough, Southern Gorda Ridge. *Economic Geology* **100**, 1135–1150.

Toulmin, P. & Barton, P. B. (1964). A thermodynamic study of pyrite and pyrrhotite. *Geochimica et Cosmochimica Acta* **56**, 227–243.

Tsujimura, T. & Kitakaze, A. (2004). New phase relations in the Cu–Fe–S system at 800°C; constraint of fractional crystallization of a sulfide liquid. *Neues Jahrbuch für Mineralogie. Monatshefte* **10**, 433–444.

Urazov, G. G. & Sokolova, M. A. (1983). The system Ag_2S–PbS. In: Brandes, E. A. (ed.) *Metals Reference Book*, 6th edn. London: Butterworths–Heinemann, 1664 pp.

Usselman, T. M. (1975). Experimental approach to the state of the core: Part I. The liquidus relations of the Fe-rich portion of the Fe–Ni–S system from 30–100 Kbars. *American Journal of Science* **275**, 278–290.

Van Hook, H. J. (1960). The ternary system Ag_2S–Bi_2S_3–PbS. *Economic Geology* **55**, 759–788.

Vokes, F. M. (1971). Some aspects of regional metamorphic mobilisation of pre-existing sulfide deposits. *Mineralium Deposita* **6**, 122–129.

Walia, D. S. & Chang, L. L. Y. (1973). Investigations in the systems PbS–Sb_2S_3–As_2S_3 and PbS–Bi_2S_3–As_2S_3. *Canadian Mineralogist* **12**, 113–119.

Walters, S. & Bailey, A. (1998). Geology and mineralization of the Cannington Ag–Pb–Zn deposit; an example of Broken Hill-type mineralization in the eastern succession, Mount Isa Inlier, Australia. *Economic Geology* **93**, 1307–1329.

Williams, P. J. (1990). The gold deposit at Calumet, Quebec (Grenville Province): an example of the problem of metamorphic versus metamorphosed ore. In: Spry, P. G. & Bryndzia, L. T. (eds) *Regional Metamorphism of Ore Deposits*. Utrecht: Coronet Books, pp. 1–25.

Wykes, J. L. & Mavrogenes, J. A. (2005). Hydrous sulfide melting: experimental evidence for the solubility of H_2O in sulfide melts. *Economic Geology* **100**, 157–164.

Yund, R. A. & Kullerud, G. (1966). Thermal stability of assemblages in the Cu–Fe–S system. *Journal of Petrology* **7**, 454–488.